DOKUZ EYLÜL UNIVERSITY

GRADUATE SCHOOL OF NATURAL AND APPLIED SCIENCES

IMPACT AND QUASI-STATIC BENDING BEHAVIORS OF SANDWICH COMPOSITE MATERIALS

by

Rifat SARIOĞLU

August, 2021

İZMİR

IMPACT AND QUASI-STATIC BENDING BEHAVIORS OF SANDWICH COMPOSITE MATERIALS

A Thesis Submitted to the
Graduate School of Natural and Applied Sciences of Dokuz Eylül University
In Partial Fulfillment of the Requirements for the Degree of Master of Science
in Mechanical Engineering, Mechanics Program

by
Rifat SARIOĞLU

August, 2021
İZMİR

M.Sc THESIS EXAMINATION RESULT FORM

We have read the thesis entitled **"IMPACT AND QUASI-STATIC BENDING BEHAVIORS OF ADHESIVELY BONDED SANDWICH COMPOSITE MATERIALS"** completed by **RİFAT SARIOĞLU** under supervision of **PROF. DR. RAMAZAN KARAKUZU** and we certify that in our opinion it is fully adequate, in scope and in quality, as a thesis for degree of Master of Science.

Prof. Dr. Ramazan KARAKUZU

Supervisor

Prof. Dr. Kutlay SEVER

(Jury Member)

Assoc. Prof. Dr. Okan ÖZDEMİR

(Jury Member)

Prof. Dr. Özgür ÖZÇELİK

Director

Graduate School of Natural and Applied Sciences

ACKNOWLEDGMENTS

First and foremost, I feel like expressing my sincere gratitude and respect to my supervisor, Prof. Dr. Ramazan KARAKUZU, for his help, excellent guidance and continuous encouragement throughout my student life at Dokuz Eylul University.

I would like to thank my colleagues, Msc.Mechanical Engineers Halis Kandaş and Samet Kıyık, who did not spare their help during my thesis and helped me in the laboratory studies.

Finally, I would like to thank my family for their support. I would not have been able to complete this thesis without the morale and motivation of my family.

Rifat SARIOĞLU

IMPACT AND QUASI-STATIC BENDING BEHAVIORS OF SANDWICH COMPOSITE MATERIALS

ABSTRACT

Composite materials are materials that are formed by the combination of two or more materials and are superior to the materials themselves. Composite materials are divided into two as matrix material and reinforcement material according to their structures. Thermoset matrices also change the mechanical structure of the composite material according to the hardener. Therefore, thermosets are widely used in aerospace industry due to their high strength.

In this study, sandwich composite was produced by vacuum assisted resin infusion method (VARIM). In the manufacturing, PVC core material with thickness of 10 mm and S2 glass fabric with areal density of 190 g/m^2 were used. For each face sheet material, S2 glass fabrics were used in three different layer numbers, four, five and six layers. First, impact tests were carried out with two different nose types as flat and hemispherical nose and impact energies of 80 J, 100 J and 120 J for three different layer numbers, 8, 10 and 12 layers. Impact tests were tested with the CEAST 9350 Fractovis Plus impact tester. After the tests, impact behaviors were examined by means of contact force-time and energy-time graphics. After the impact test, the damage photos of the samples are given in the figures. Then quasi-static punch shear test was applied to sandwich composite by using the Universal Shimadzu Test machine with both penetrators of flat and hemispherical noses and punch shear test fixture. The tests are performed at five different crosshead speeds, in three different layers, 8, 10 and 12 layers, and in three repeats for each test. After the experiments, force-deflection diagrams were drawn and results were compared with each other. In addition, quasi-static damage photos of the samples were visually examined.

Keywords: Low velocity impact, quasi-static punch, vacuum assisted resin infusion method, S2 glass/epoxy

SANDVİÇ KOMPOZİT MALZEMELERİN DARBE VE YARI-STATİK EĞİLME DAVRANIŞLARI

ÖZ

Kompozit malzemeler, iki veya daha fazla malzemenin bir araya gelmesiyle oluşan ve malzemelerin kendisinden üstün olan malzemelerdir Kompozit malzemeler yapılarına göre matris malzemesi ve takviye malzemesi olarak ikiye ayrılır. Termoset matrisler, sertleştiriye göre kompozit malzemenin mekanik yapısını da değiştirir. Bu nedenle termosetler, yüksek mukavemetleri nedeniyle havacılık endüstrisinde yaygın olarak kullanılmaktadır.

Bu çalışmada, vakum destekli reçine infüzyon yöntemi (VARIM) ile sandviç kompozit üretilmiştir. İmalatta 10 mm kalınlığında PVC çekirdek malzeme ve 190 g/m2 alan yoğunluğunda S2 cam kumaş kullanılmıştır. Her bir yüzey tabakası malzemesi için dört, beş ve altı katman olmak üzere üç farklı katman sayısında S2 cam kumaşları kullanılmıştır. İlk olarak, düz ve yarım küre burun olmak üzere iki farklı burun tipi ve 80 J, 100 J ve 120 J darbe enerjileri ile üç farklı katman sayısı, 8, 10 ve 12 katman için darbe testleri gerçekleştirilmiştir. Darbe testleri, CEAST 9350 Fractovis Plus darbe test cihazı ile test edilmiştir. Testler sonrasında temas kuvveti-zaman ve enerji-zaman grafikleri ile darbe davranışları incelenmiştir. Darbe testi sonrasında numunelerin hasar fotoğrafları şekillerde verilmiştir. Daha sonra, hem düz hem de yarım küre uç girişleri ve zımba kesme testi fikstürü ile Universal Shimadzu Test makinesi kullanılarak sandviç kompozite yarı statik kesme testi uygulandı. Testler, beş farklı hızda, üç farklı katmanda, 8, 10 ve 12 katmanda ve her test için üç tekrarda gerçekleştirilir. Deneyler sonrasında kuvvet-sehim diyagramları çizilmiş ve sonuçlar birbirleriyle karşılaştırılmıştır. Ayrıca numunelerin Yarı Statik hasar fotoğrafları görsel olarak incelenmiştir.

Anahtar kelimeler: Düşük hızlı darbe, yarı statik kesme, vakum destekli reçine infüzyonu metodu, S2 cam/epoksi

CONTENTS

Page

M.Sc THESIS EXAMINATION RESULT FORM ii
ACKNOWLEDGMENTS iv
ABSTRACT iv
ÖZ vi
LIST OF FIGURES viii
LIST OF TABLES x

CHAPTER ONE - INTRODUCTION 1

CHAPTER TWO - COMPOSITE MATERIALS 10

2.2 Classification of Composites According to Matrix Materials 10
2.2.1 Metal Matrix Composites 10
2.2.2 Ceramic Matrix Composites 11
2.2.3 Polymer Matrix Composite 12
2.2.3.1 Thermosets 13
2.2.3.2 Thermoplastics 13
2.3 Classification of Composites According to Reinforcement Materials 14
2.3.1 Fiber Reinforced Composites 14
2.3.2 Particulate Composites 15
2.3.3 Laminated Composites 15
2.4 Sandwich Composites 15
2.4.1 Definition 16
2.4.1.1 Face-sheet 16
2.4.1.2 Core Material 16
2.4.1.3 Adhesives 17
2.4.1.3.1 Epoxy. 17
2.4.1.3.2 Polyesters 17
2.4.1.3.3 Fenols. 18
2.4.1 Advantages and Disadvantages of Sandwich Composite 18

CHAPTER THREE - MATERIALS AND METHOD 19

3.1 Vacuum Assisted Resin Infusion Molding 19
3.2 Quasi- Static Punch Shear Test 21
3.3 Low Velocity Impact Test 23

CHAPTER FOUR - RESULTS AND DISCUSSION 25

4.1 Impact Results 26
4.1.1 Contact Force Results 26
4.1.2 Absorbed Energy 35
4.1.3 Impact Damage 45
4.2 Quasi-Static Test Results 48
4.2.1 Force-Displacement Results 49
4.2.2 Quasi-Static Damage 57

CHAPTER FIVE - CONCLUSION 61

REFERENCES 63

LIST OF FIGURES

Page

Figure 2.1 Electronic component from metal matrix composite..... 11
Figure 2.2 Exhaust nozzle made of ceramic matrix composite 12
Figure 2.3 Structure of the polymer molecule 12
Figure 2.4 Schematic representation of (a) thermoplastic polymer and (b) thermoset polymer 14
Figure 2.5 Sandwich composite structure 16
Figure 3.1 Schematic illustration of the vacuum assisted resin infusion molding (VARIM) process..... 19
Figure.3.2 a) S2 glass fabrics on mold release agent on, b) PVC foam is placed on S2 glass fabrics, c) resin dispersant placed on the peel ply, d) whole system covered with vacuum bag 20
Figure 3.3 Wet saw to aid in cutting specimens..... 21
Figure 3.4 Test specimen with100mmx100mm dimensions 21
Figure 3.5 Specimen attached to punch shear apparatus..... 22
Figure 3.6 Test machine with punch-shear test apparatus 23
Figure 3.7 a) CEAST Fractovis Plus impact test machine, b) test specimen..... 24
Figure 4.1 Force-time graphics of samples with 10-ply for hemispherical nose and 100J energy 26
Figure 4.2 Contact force-time graphs according to the impact energy for different ply and impactor noses..... 28
Figure 4.3 Contact force-time graphs according to the number of ply for different energy levels and impactor noses..... 30
Figure 4.4 Contact force-time graphs according to impactor noses types for different energy levels and number of ply 32
Figure 4.5 Contact force-velocity graphs according to the number of ply for energy levels and impactor noses..... 35
Figure 4.6 Definition of the impact energy of the 8-layer sandwich composite tested with a flat nose and 120J energy, energy absorbed in the energy-time graph..... 36

Figure 4.7 Energy-time graphs depending on energy change 38
Figure 4.8 Energy-time graphs due to number of ply 39
Figure 4.9 Energy-time graphs due to impactor noses 41
Figure 4.10 Power-velocity graphs according to number of ply and impactor noses 42
Figure 4.11 Power-time graphs depending on energy change 43
Figure 4.12 Power-time graphs due to number of ply 44
Figure 4.13 Power-time graphs due to impactor noses 45
Figure 4.14 Impact damages types of sandwich composite samples with flat and hemispherical noses at different impact energies at 8 ply 46
Figure 4.15 Impact damages types of sandwich composite samples with flat and hemispherical noses at different impact energies at 10 ply 46
Figure 4.16 Impact damages types of sandwich composite samples with flat and hemispherical noses at different impact energies at 12 ply 47
Figure 4.17 Quasi-static test results of samples with 10 layer subjected to hemispherical nose and 5different speeds 49
Figure 4.18 Force-displacement graphs according to the various crosshead speeds for different ply and noses 51
Figure 4.19 Force-displacement graphs according to the number of ply for different crosshead speeds and noses 52
Figure 4.20 Force-displacement graphs according to the noses for different crosshead speeds and ply 54
Figure 4.21 Force-speed graphs according to the noses for different ply 56
Figure 4.22 Damage after quasi-static test of 8-ply flat, hemispherical noses and sandwich composite samples at different speeds 58
Figure 4.23 Damage after quasi-static test of 10-ply flat, hemispherical noses and sandwich composite samples at different speeds 59
Figure 4.24 Damage after quasi-static test of 12-ply flat, hemispherical noses and sandwich composite samples at different speeds 60

LIST OF TABLES

Page

Table 4.1 Low velocity impact test results for different number of layers, nose types and energies..... 33

Table 4.2 Composite applied power results for different number of layers, nose types and energies..... 42

Table 4.3 Maximum forces and absorbed energies of quasi-static test for 8 ply, 10 ply and 12 ply specimens at different speeds and noses 50

CHAPTER ONE
INTRODUCTION

Composite materials are materials that are formed by the combination of two or more materials and are superior to the materials themselves. Composite materials are divided into two as matrix material and reinforcement material according to their structures. According to their matrices, composites are divided into three as metal matrix, ceramic matrix and polymer matrix. Although various composite types are used today, the most used composite types are those with polymeric matrix structure.

Polymeric matrix types are divided into two as thermoset and thermoplastic matrices. Thermoset matrix type was used in this academic study. Thermoset matrices also change the mechanical structure of the composite material according to the hardener material.

In addition, composite materials are divided into four according to the placement of reinforcement elements and their shapes. These are particulate composites, layered composites, sandwich composites and fiber composites. In this study, sandwich composite, is one of the oldest and most widely used layered composite type, has been studied.

The usage of sandwich composites is increasing in the aviation, defense and space industries as technology is developing day by day. The purpose of use of these materials is that they are lighter in weight than other materials in nature and their resistance to external loads is quite high.

Sandwich composites consist of a lightweight core in the middle and a face-sheet that will carry the load and pressure loads on both surfaces of the core and an adhesive layer that connects these two elements.

Schubel et al. (2005) studied the low velocity impact behavior of a sandwich composite material consisting of a carbon epoxy surface layer PVC foam. It has been found that the load contact properties of the composite material are similar

between low speed impact behavior and semi-static loading. Therefore, the low speed impact event was assumed as the quasi-static loading behavior. Therefore, the ease of use of the quasi-static test has been determined in order to predict the impact response and to be easily resolved.

Zhou et al. (2012), the purpose of doing this is to compare the puncture strength of sandwich composites experimentally and numerically and to model the low velocity impact test. As a result of the researches, the experimental results and the numerical results overlapped with each other. It was determined that the puncture resistance of crosslinked PVC foams was higher than the puncture resistance of flat bonded PVC foams.

Gustin, et al. (2005) experimentally investigated the impact and post-impact mechanical properties of a sandwich composite produced as a carbon fiber Kevlar hybrid. As a result of the work done, adding Kevlar material to the surface layer increased the absorbed energy and maximum contact force by ten percent compared to the carbonfiber surface layers. The addition of Kevlar surface layer to the material showed a decrease in the modulus of elasticity in the composite material.

Al-Shamary et al. (2016) to examine the cores of sandwich composites with different foam configurations using low speed impact test. It was aimed to determine the absorbed energy, contact forces and displacements at different energy levels. In the light of the experiments, as a result of the increase in impact energy, separations between fiber breakages, core damage and fiber epoxy were observed in the surface layers. Indentation damage was clearly seen in the sandwich composite with the increasing thickness of the samples.

Doğan & Arıkan (2017) conducted an experimental study with low speed impact test of thermoset and thermoplastic surface layer sandwich composites. E-Glass has been chosen as the PVC foam surface layer as the core material. Although thermoset is chosen as a matrix and as a thermoplastic, matrices that are the combination of the two are also used. Impact tested at low speed at various energy levels. As a result of this study, it was found that bending stiffness of thermoset sandwich composites is

higher than thermoplastic sandwich composites. However, it has been observed that the load carrying capacity of the sandwich composites consisting of thermoplastic matrix is high in the surface layers. High contact force and low deformation were observed in sandwich composites consisting of thermoset surface layer.

Ude et al. (2013) conducted an experimental research with low velocity impact test of surface layers consisting of woven natural silk fiber and sandwich composites produced with honeycomb, foam and coremat materials as core materials.. In the tests, the energy absorption capacity was higher in epoxy and foam samples. It was found that the least deflection composite material type was sandwich composite consisting of honeycomb core. It was observed that the most damaged ones were coremat and composite materials with epoxy content.

Anderson & Madenci (2000) in this academic study, the force indent response of sandwich panels with a rigid spherical tip was studied. As core material polymethacrylimide foam was used. Graphite/epoxy / is used as the surface layer. It is aimed to develop a three-dimensional solution for the contact pressure applied by the rigid spherical tip to the sandwich panel. The quasi-static indentation test was also performed to verify the analytical solution. When looking at the results, the data obtained until the damage of the core and surface layers coincide with the numerical data.

Jordan et al. (2013) low velocity impact and high velocity impact tests were performed to determine the material properties of E-glass and phenolic composites. In order to perform the high velocity impact test, the mechanical properties of the materials were investigated by making semi-static shear tests by approaching it.

Hazizan & Cantwell (2002) studied the low speed impact effect of sandwich composites whose core material is foam. Core materials PVC, PUR foam were used. Woven glass fiber was used as the surface layer material. In the researches, it was seen that the shear modulus increased with the increase of the impact force. It has been found that the impact behavior depends on the elastic property of the core material of the sandwich composite. The first damage to low-density foams was seen

as shear damage. Damage to the surface layer was seen as delamination in sandwich structures with high shear modulus.

Ozdemir et al. (2014) examined the low speed impact behavior of core materials of different thicknesses. PVC and PET foam were selected as core materials and their thickness was determined as 5, 10 and 15 mm. E-Glass material was chosen as the surface material and three layers were chosen as the number of layers. [$\pm$45º/0º/90º/core/90º/0º/$\mp$45º]. As a result of the studies, it was observed that the contact strength decreased with the increase of core thickness. As the core thickness increased, the amount of energy absorbed increased. It was found that the bending stiffness of the samples made of PET foam was minimum and the flexural rigidity of the samples made of PVC foam was maximum.

Feng & Aymerich (2020) studied the impact energy response of PVC foam with different densities. Carbon / epoxy was used as the surface layer material and sandwich composites were produced using two different orientation sequences. These orientation sequences are $[0/90_3/0]$, $[0_3/\pm45]_s$. It has been found that the energy expended at the time of impact is independent of the core density. It has been found that the damage area decreases with the increase of core density at high energies in sandwich panels with $[03/\pm45]_s$ orientation. [0/903/0], $[03 / \pm 45]_s$ orientation and the damage resistance of the core density on the sandwich composite have been linked to the bending stiffness of the surface layers in the sandwich composite.

Ataş & Sevim (2010) examined the low speed impact behavior of sandwich composites with balsa wood core and PVC foam core. E-Glass is used as the surface layer material. Testing has been applied to composite materials at various energy levels. As a result of the study, it was observed that sandwich composite with balsa wood core is more rigid than sandwich composite with PVC foam. Therefore, it was concluded that PVC foams undergo further deformation. Since the adhesion behavior of sandwich composites with PVC core with the surface layer is high with the increase of impact energy, fiber breakage occurred less than sandwich composites with balsa wood core.

Saklya et al. (2016) studied the behavior of sandwich composites used in railway structures in low speed impact testing. PET foam and PES foam are used as core materials. E-glass was used as the surface layer. 24 layers of E glass were used in the composite using PES foam. 20 layers were used in PET foam. In the light of the tests, matrix damage and delamination were determined as the main damages. Cavitation was detected at a small distance in the impact area of the tested samples and this has been found to remove the bending energy.

Balaban et al. (2019), sandwich composite with PVC foam surface layer E-Glass as core material was produced. In this sandwich composite, the thickness of the lower surface layer and the upper surface layer was produced differently, and the low speed impact behavior of this sandwich structure was investigated. Tests were carried out at 4 different energy levels as 20J, 40,60J, 80J. As a result of the tests, fiber breakage and matrix cracks were observed at low energy levels. At the tested energy levels, only the top surface layer was damaged, and it was found that the impactor stopped in the core or sub-surface layer. As the impact energy increased, the area of damage in the material expanded.

Bulut & Erklig (2018), by developing a low velocity impact test on hybrid composites made of three different fiber types, namely Carbon, Kevlar and S-glass, quasi-static indentation was determined, and it was aimed to learn the energy absorption and load carrying capacity of the composites. As a result of the work carried out, the indentations around the lead reduced its load carrying capacity and caused the initiation of fiber breakage, delamination and matrix cracking. S-Glass reinforced composites have been found to have a weak indentation resistance and damage tolerance, which can be enhanced by carbon, Kevlar hybridization.

Sadeghi & Houssein (2017), indentation geometry and quasi-static punch shear properties of glass/epoxy laminated composites of the weight percentage of carbon nanotubes were experimentally studied. S-glass fabric has been chosen as the facesheet materials. In the study, a quasi-static test was carried out with three different tips: flat tip, conical tip and ogive tip. As a result of the experiments, the greatest effect on the energy absorption of carbon nanotubes is the draw-shear area.

In comparison between the ends, the greatest contact force to the nanotubes was obtained by hitting the flat tip, and it was found that the greatest energy absorption belongs to the conical tip. In smooth specimens, the largest and smallest contact force belongs to the flat, ogive tip, while the largest and smallest energy absorption belongs to the conical and flat tip, respectively.

Lin & Fat (2006), a study has been carried out on the quasi-static punch shear test in order to determine the damage that will occur during the impact event of the composite material consisting of carbon / epoxy. A comparison was made with the finite element program to ensure the accuracy of the results in experimental studies. As a result of the study, it was found that the matrix cracks occurred between the die and the punch due to the high transverse shear stress. With the increase of the load, the cracks spread in the matrix as intralaminar or laminar cracks. Interlaminar cracks caused delamination at the interface, which showed a decrease in structural rigidity.

Ayten et al. (2019), quasi-static punch shear of aramid epoxy composites of different thicknesses has been studied both experimentally and numerically. As a result of this study, the maximum contact force was found at the lowest aperture drilling rate, while the highest slope was found at the highest aperture drilling rate. It has also been found that as the aperture penetration rate increases, the damage mode changes from dominant shear damage to dominant bending damage.

Xiao et al. (2005), LS DYNA can be performed for PW S-2 glass / SC-15 epoxy composite material and damage characterization through punch-shear tests and simulations. In other words, as the final thickness of the samples increased, the bending stiffness of the sandwich composite was increased and indentation failure was more clearly observed. One-core samples at 40 J at maximum contact force are about 177% higher than three-core samples.

Yahaya et al. (2014) designed Kenaf/Kevlar hybrid composites and experimentally studied their response to semi-static penetration and high velocity impact testing. In this study, hybrid composites absorbed more penetration energy than kevlar/epoxy and kenaf/epoxy composites. Hybrid composites with kenaf in the

innermost layers (Kevlar in the outer layers) gave maximum penetration force and energy absorption. Specific energy absorption (energy absorption per area density) is higher in Kevlar/epoxy than hybrid and kenaf/epoxy composites.

Experimentally studied the behavior of quasi-static loading by adding an extra layer on top of the sandwich composite and with the difference of lower and upper core types. PUR foam and PVC foam are used as core materials. E-glass is used as the surface layer. In the experiments made for both core types, it was determined that the hardness of the upper composite increases when the thickness of the core decreases. The upper surface layer and the inner surface layer were damaged at low loads. In the tests performed, it was concluded that PVC foam undergoes less deformation than PUR foam in the experiments conducted with the sandwich composite consisting of PVC foam on the top in multi-layer sandwich composite because the PVC foam is rigid than PUR foam (Salami, 2013).

Önder & Robinson (2019) examined the impact behavior of the material by performing a quasi-static test of sandwich composites used in high-speed train wagons. PET foam was used as core material. E-Glass was used as the surface layer material. Experimental studies were verified by finite element analysis method. Various damage modes, impact resistance performance were determined in sandwich composite materials. Penetration resistance was verified with the finite element program.

Shuaeib & Soden (1997) experimentally and theoretically studied the semi-static indentation damage of a sandwich beam whose core material is PVC foam surface layer E-glass. Cylindrical tip is used as the working end. As a result of the study, a harmony has been achieved between elastic, elasto-plastic methods and experimental damage loads. The load on the sandwich beam exhibited an elastic-plastic behavior in the core region, and elastic bending behavior was observed in the upper surface layer. It has been determined that there is a link between these behaviors.

Fernandes et al. (2016) studied the ballistic effect and quasi-static punch shear behavior of fiberglass polymer composites. In quasi-static punch shear tests applied

to the material, failure modes such as internal damage, fiber and matrix rupture, matrix cracking and delamination were observed in composites.

Liang et al. (2014), 8 satin woven tile epoxy composites were produced and tested under different loads. In addition, the experimental results were compared with the results obtained from the finite element analysis program. As a test, the semi-static puncture test was performed and the damage and penetration analysis was performed. As a result of researches, matrix cracks start between punch and die due to high shear stress. As the loads increase, the cracks between laminate also increase. It has also been observed that as shear stress increases, it turns into bending stress. Fiber breakage also occurred due to the increase in bending stress.

Flores-Johnson & Li (2011) presents studies on semi-static indentation testing of sandwich panels consisting of carbon fiber surface layer and polymeric core with various geometric noses. As a result of the experiments, it has been determined that the energy absorbed in the indentation in the damage area is effective on both the geometric tip type and core density. In the panels subjected to the experiment, surface layer core separation and surface layer core damage were observed. It has been found that the indentation load varies with the distance between the support plates.

Reddy et al. (1998), the quasi-static low speed impact tests of the sandwich composite, the core material of which consists of PVC foam, the surface material E-glass, have been performed. Conical and hemispherical ends are selected as the end to be impact tested. In the light of the researches, as a result of the experiments on sandwich composites with foam cores, the perforation and penetration energy equations of the sandwich structures with quasi static loading with the conical end were derived. In the quasi-static and low velocity impact tests performed on sandwich composites, it was observed that the damage mechanism was in the core. The thickness and density of the core is an important factor in the damage mechanism. Surface layers have been found to play an important role in absorbing energy. It has been seen that the energy relations obtained for the hemispherical end are also available for the conical end.

When the studies are examined, it is seen that E-glass and carbon fiber are used as surface layer in sandwich composite materials. However, S-Glass was not used as the surface layer in any of the studies. The aim of the study is to investigate experimentally the absorbed energy capacity of the sandwich composite by quasi-static test on a sandwich composite material with a polyvinyl chloride core with different numbers of S-Glass layers at five various crosshead speeds with two different noses. Force-deformation curves are drawn and analyzed. Then, the energy absorption capacity was examined by performing a low speed impact test at three different energy levels with the materials in the same layer. After this test, force-time, energy-time graphs are drawn and interpreted.

CHAPTER TWO
COMPOSITE MATERIALS

2.1 Introduction

Composite materials are materials that have higher mechanical properties than those obtained by the combination of two or more materials. Composite materials consist of two components, matrix and fiber. The advantages of composite materials are high strength, low weight and high rigidity. There are three types: ceramic, polymer and metallic matrix. The rigidity and strength of polymer matrices are low. The strength of metal matrices is ductile. Ceramic matrices are fragile and hard resistant.. The task of the matrix is to keep the fibers in proper spacing and direction. The reinforcement stage is the part that adds rigid and strength to the material. Reinforcement materials consist of fabric and particles. Often reinforcement materials are more durable and rigid than matrix materials (Campbell, 2010).

2.2 Classification of Composites According to Matrix Materials

The matrix material in the composite material can be ceramic, metal and polymer matrix. According to the matrix material used, composite materials are divided into three as ceramic matrix composites (CMC), metal matrix composites (MMC) and polymer matrix composites (PMC). Although polymer matrix composites are widely used in the industry, ceramic matrix and metal matrix composites are also used in applications where high temperature resistance is required (Mallick, 2007).

2.2.1 Metal Matrix Composites

Metal matrix composites have advantages such as high temperature resistance, high strength and modulus, high wear resistance and low expansion coefficient compared to metals. They are less commercially used due to their high cost and usage areas. Discontinuous reinforced metal matrix composites have some limited

uses. For continuously reinforced metal matrix composites there are hardly any valid applications (Campbell, 2010).

Due to their high mechanical properties, the use of metal matrix composites in aerospace, aerospace and automotive industries is increasing day by day.

Therefore, the development and increase of production methods of metal matrix composites has increased the demand for such composites (Balasubramanian, 2013).

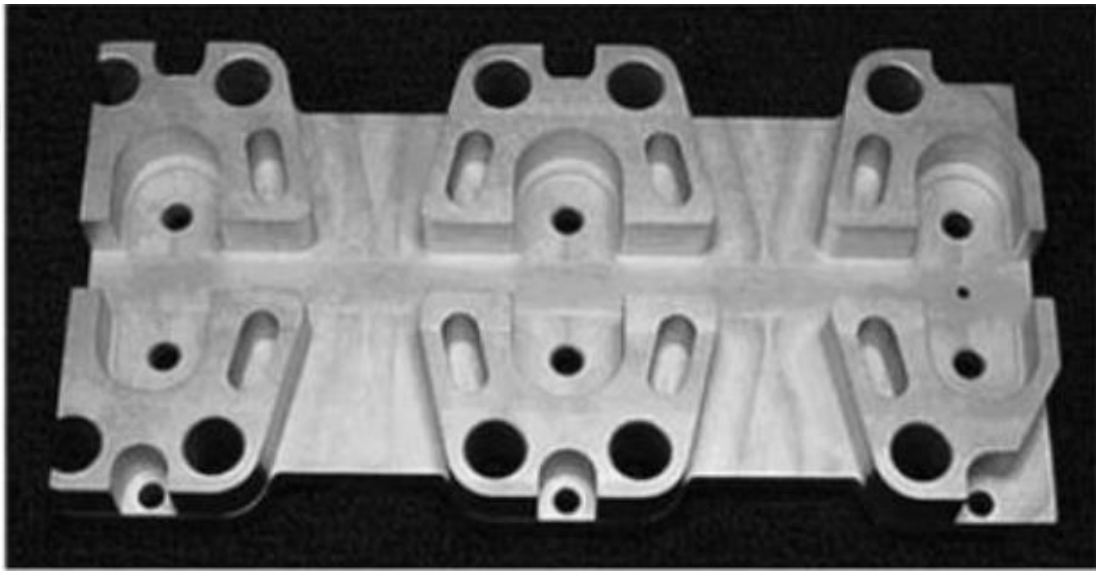


Figure 2.1 Electronic component from metal matrix composite (Campbell, 2010)

2.2.2 Ceramic Matrix Composites

Ceramic matrices are used in the aerospace industry because of their high temperature resistance, high compression strength, and high corrosion resistance. Fiber, whiskers and particles are used in metal, polymer matrix composites to reinforce the composite, while in ceramic matrix composites they are used to increase toughness. Ceramic matrices were first used in the form of Carbon-Carbon composites in aircraft brake discs, rocket nozzles, heat shields and racing car brakes Later, combustion chambers and energy generation components such as turbines, burners and heat recovery systems were developed (Campbell, 2010).



Figure 2.2 Exhaust nozzle made of ceramic matrix composite (Campbell, 2010)

2.2.3 Polymer Matrix Composite

Polymeric materials are molecules with a similar chemical structure formed by the combination of multiple covalent bonds.

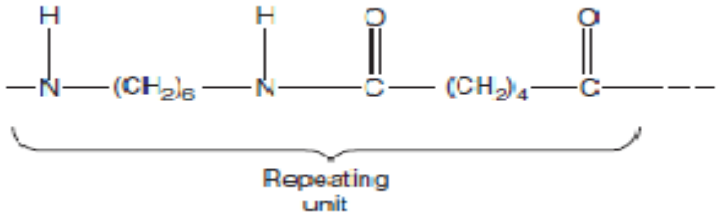


Figure 2.3 Structure of the polymer molecule (Mallick, 2007)

The most commonly used composites are polymer matrix composites. It is widely used due to its low cost, simple production methods and high strength. Its disadvantages are low operating temperature, low thermal, moisture expansion and low elasticity (Kaw, 2006).

Polymeric matrix composites are divided into thermoset and thermoplastic due to different chemical bonds.

2.2.3.1 Thermosets

Thermosets are plastic materials that harden easily below room temperature. Therefore, it cannot be melted and used again after hardening. In the cured state, they form a three-dimensional molecular chain. This formed chain is called cross linking. Thermoset materials have high thermal and dimensional stability. Its high electrical, chemical and solvent resistance is among its properties. Thermoset materials have to be used with a hardener since their structure is fragile materials. Commonly used types are epoxy, vinylester, phenolics and polyimides (Mazumdar, 2002)

2.2.3.2 Thermoplastics

Thermoplastic materials are harder than thermoset materials, but generally the material is ductile. Since there are no cross-links in thermoplastic materials, they can be reshaped by reheating. Thermoplastic materials should also be used with reinforcement elements due to their low strength and hardness properties. In case of damage, thermoplastic materials are easier to repair or to bond with another part compared to thermoset materials. Thermoplastics show creep resistance at higher temperatures than thermosets. Polyethylene, polypropylene, nylon and polycarbonate can be shown as the thermoplastic materials used (Mazumdar, 2002).

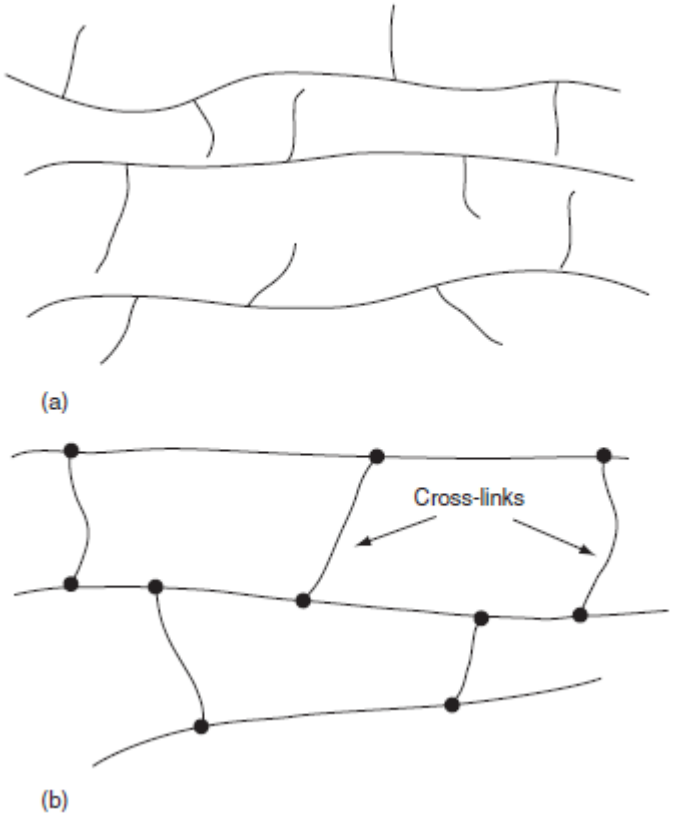


Figure 2.4 Schematic representation of (a) thermoplastic polymer and (b) thermoset polymer (Mallick, 2007)

2.3 Classification of Composites According to Reinforcement Materials

The reinforcement materials used in composite materials are divided according to their size and orientation. These are fiber reinforced composites, laminated composites, particulate composites and hybrid composites (Staab, 2015).

2.3.1 Fiber Reinforced Composites

The mechanical properties of the composite structures vary according to the length of the fibers in the matrix. Composite materials are divided into long fiber composites and short fiber composites. The fiber orientations of long fiber composite materials can be placed in one or two directions. Therefore, the charge transfer in the matrix becomes easier. Short-fiber composites are carried intermittently from the

matrix due to the short length of the fibers, and thus cracks may occur in the matrix. (Rajak et al., 2019).

2.3.2 Particulate Composites

Particulate composite material consisting of particles suspended in the matrix. Particles have a variety of shapes, sizes. They are used for many applications where the strength parameter is not important (Staab, 2015).

2.3.3 Laminated Composites

Laminated composite is a type of composite formed by arranging a series of layers in the direction of the layer. For example, structures such as leaf spring suspension in automobiles are made of laminated composite and are exposed to loads such as bending and torsion. Therefore, it is necessary to know the mechanical properties of the laminas such as stress and strain in the design of such structures. If the composite material consists of more than one different lamina or fibers, it is called hybrid composite (Kaw, 2006).

2.4 Sandwich Composites

Sandwich structures first appeared on the fuselage and wings of warplanes in World War II. Balsa wood was used as the core material and wood veneer was used as the surface material. Various improvements to the core material were first considered in the development of sandwich structures after the end of World War II. These are honeycomb structures with various cellular structures and plastic materials that are easy to obtain, lightweight and durable in terms of strength have begun to be used (Anonymous, 2003a).

Nowadays, sandwich composites are used in aerospace and automotive industries with their properties such as low density and high bending strength (Foo et al., 2006).

2.4.1 Definition

Sandwich composite structurally consists of two face sheets made of metal or fiber and these face sheets are bonded to the light and thick material called the core with an adhesive (Carlsson & Kardomateas, 2011).

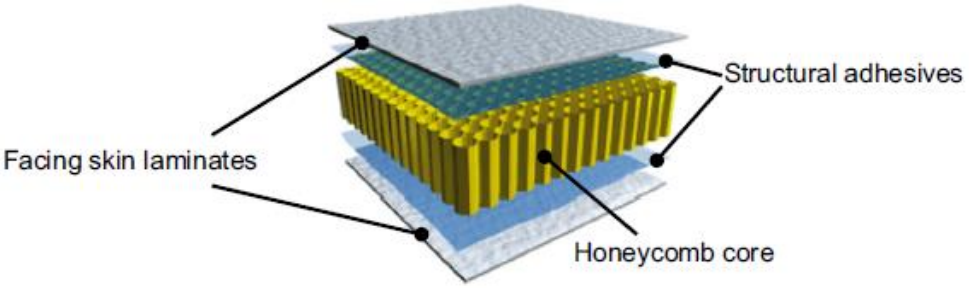


Figure 2.5 Sandwich composite Structure (Rana &Fanguerio, 2016)

2.4.1.1 Face-sheet

Face-sheet serves more than one purpose by varying depending on sectoral applications. Generally, it is the part that carries bending loads (lower surface tries to compress, upper surface tries to pull) or shear stress loads in plane. Fiber reinforced plastics as the face sheet material, titanium aluminum and steel as metal are widely used. The materials used as the face sheet are quite high. The reason for the widespread use of polymer face sheets is their high strength and low density. In addition, the use of polymer reinforcements both as a face sheet and as a core is among the advantages (Gupta, 2003).

In this thesis, S-Glass/epoxy was used as the face sheet.

2.4.1.2 Core Material

The task of the core material in sandwich composites is to bear the bending, shear forces, and to separate the surface layers. In addition, it is to separate the two surface

layers with adhesives and to make the load transfer between the surface layers properly. Polymeric foams, balsa wood and honeycomb structures are used in core material (Rana & Fanguerio, 2016).

Honeycomb core is a structure formed by the combination of multiple cellular structures. Honeycomb nuclei can be produced by changing the spaces between cells, cell sizes and shapes, and various new nuclei types. Among the properties of these cores, they are flexible, light and have a high impact resistance. These structures are generally made of materials such as stainless steel, refractory metals, resin dipped paper, etc. It is used in aviation, space, maritime industries (Rana & Fanguerio, 2016).

Foam cores have been used due to the excess weight and moisture absorption problems created by natural core materials. It is used in aviation and maritime applications since its production costs are cheaper than honeycomb cores. Thermal insulation of foam cores is higher than honeycomb cores (SAE, 2013).

2.4.1.3 Adhesives

Adhesives combine the surface layers with the core. It is responsible for the balanced transmission of shear and tear forces between the surface layers and the core, and allows the materials to work together as a structure. Adhesives are divided according to their chemical structures (SAE, 2013).

2.4.1.3.1 Epoxy. In the thermoset resin class, material joining is the most used adhesive. It is widely used in composite manufacturing applications. Epoxies are known for their high modulus of strength, low volatile matter levels, low hardening shrinkage and good chemical resistance. It has excellent adhesion properties due to its easy processing and high adhesion strength. Its disadvantages are its brittleness in a short time and its adhesion to decrease when exposed to moisture (SAE, 2013).

2.4.1.3.2 Polyesters. Polyesters are cheap and chemically reactive adhesive types compared to epoxy resins. Polyesters are resistant to UV, rays and fatigue resistance.

There is no decrease in its performance in a humid environment and its compatibility with glass fiber is high. It is used in the maritime and energy sectors (SAE, 2013).

2.4.1.3.3 Fenols. Phenols are a type of thermoset used in applications requiring high fire resistance temperature performance and long-term durability Phenolics are used in aerospace and aviation industries due to their high fire resistance (SAE, 2013). The disadvantages of phenols are that they are volatile during curing and form a porous structure in the absence of high pressure (Balasubramanian, 2013).

2.4.1 Advantages and Disadvantages of Sandwich Composite

Properties such as bending stiffness, high strength, high vibration damping and lightness are among the advantages of sandwich composite. The disadvantages of sandwich composites are high production costs, difficult repairs of damaged parts, and high thickness of the materials produced (Gupta, 2003).

CHAPTER THREE
MATERIALS AND METHOD

3.1 Vacuum Assisted Resin Infusion Molding

In this study, sandwich composite was manufacutered by vacuum asissted resin infusion moulding method (VARIM). VARIM method is made of glass fiber, carbon, aramid etc. in a mold with a mold release agent. Vacuum paste and vacuum bag placed around the molds of the fibers, and these fabrics are placed in accordance with the designed layer arrangement. It is to isolate the material from the external environment by means of the vacuum, and then the resin is injected (Goren & Atas, 2008). Schematic representation of the method is given in the figure 3.1.The process steps related to this process are explained in detail below.

In the study Polyurethane core foam (AIREX C71.55 PVC Foam) is used as core material. Three different types of S-Glass are used, with 8, 10 and 12 layers on the surface layers. Epoxy resin and adhesive are used to bond the surface layers and core material to each other.

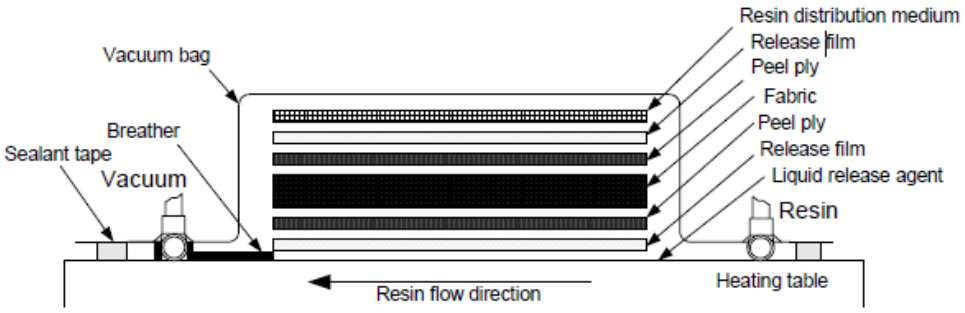


Figure 3.1 Schematic illustration of the vacuum assisted resin infusion molding (VARIM) process (Ataş & Gören, 2008)

1) The peel paper is placed neatly on the device.
2) It is conveniently placed on fabrics and foam peeling paper..
3) The resin dispersing net and fabric are laid on the placed fabrics.

4) Distributor pipes are placed on the net and the fabric is covered with a vacuum bag sealing paste.
5) One side of the pipes is tightened with a clamp and the other side is connected to the vacuum and the air in the vacuum bag is vacuumed.
6) The hardening resin mixture is brought into a chamber and the squeezed pipe is loosened and dipped into the chamber and the fabrics are impregnated with the resin.
7) Impregnated fabrics are pre-cured at 50 ° C for 30 minutes. It then continues with a second curing at 80 ° C for 8 hours. It is obtained by removing the material after the curing process is completed.

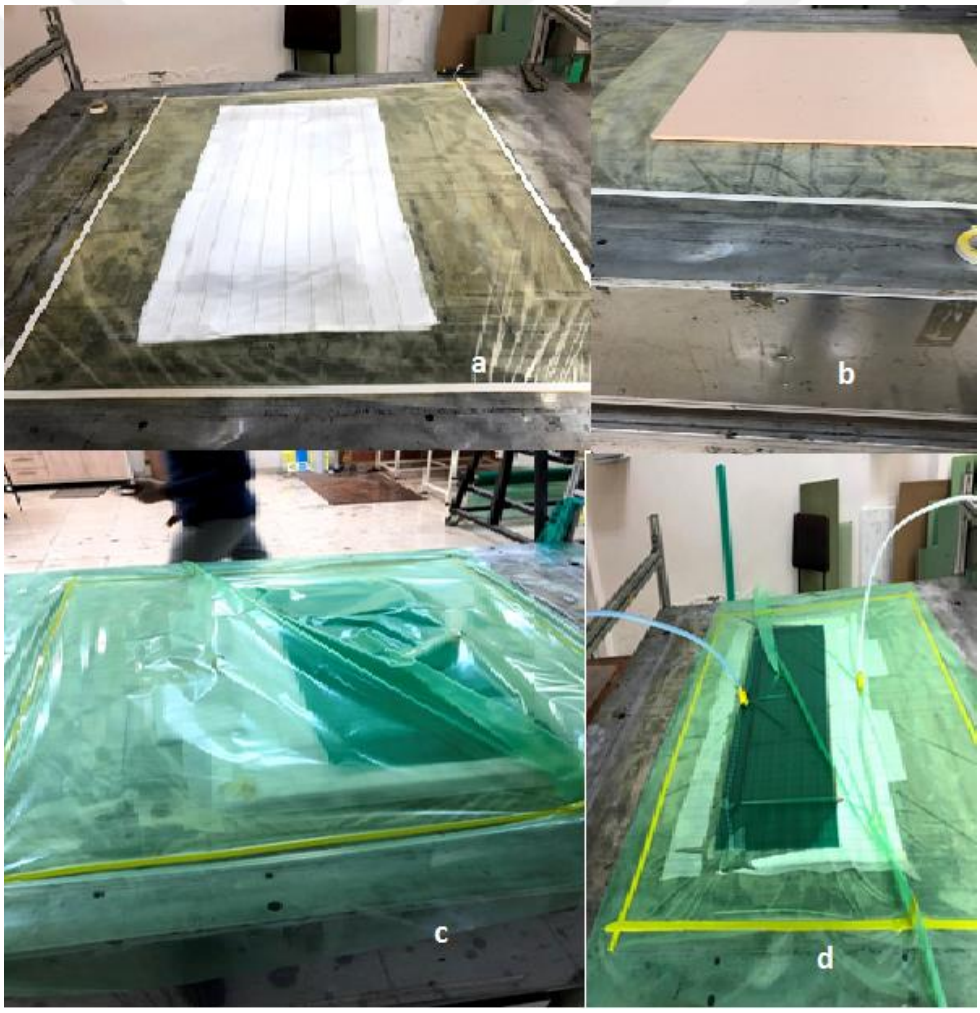


Figure.3.2 a) S2 glass fabrics on mold release agent on, b) PVC foam is placed on S2 glass fabrics, c) resin dispersant placed on the peel ply, d) whole system covered with vacuum bag (Personal archive, 2021)

Wet saw is used to cut S2 glass PVC sandwich composite material into 100mm x 100mm pieces.



Figure 3.3 Wet saw to aid in cutting specimens (Personal archive, 2021)



Figure 3.4 Test specimen with 100mmx100mm dimensions (Personal archive, 2021)

3.2 Quasi- Static Punch Shear Test

In the researches, it was concluded that the results of the damage modes of the quasi-static punch tests are similar to the results of the high speed ballistic impact test and that the high speed ballistic impact test can be modeled according to the

quasi-static punch test. The main damage mechanisms of the quasi-static test are fiber breakage, hole expansion and crack propagation (Abrate, 2011).

In addition, it has been suggested that the damage mechanism in the high speed impact test is the same as the findings in the quasi-static puncture test. The displacement level of each damage is considered comparable for both static and dynamic situations (Xiao et al., 2007).

The purpose of our quasi-static punch shear test is to measure the indentation resistance of the material and learn its energy absorption. Quasi-static punch shear test apparatus consists of a 76 mm diameter hole in the middle, a 12.7 mm thick 100x100 mm square plate and a 50-80 mm thick support piece. The sample we will test is placed between the apparatus as shown in the figure and mounted by tightening with 8 bolts around it.

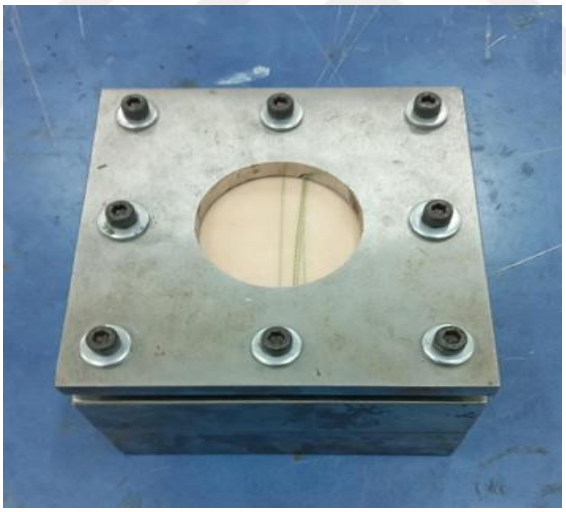


Figure 3.5 Specimen attached to punch shear apparatus (Personal archive, 2021)

The diameter of the tips to be tested is 12.7 mm and the tests are carried out with straight and hemispherical tips, with 3 repetitions at 5 different speeds of 1 mm/min, 5 mm/min, 15 mm/min, 25 mm/min and 50 mm/min. There was no dynamic effect on the material during the tests.

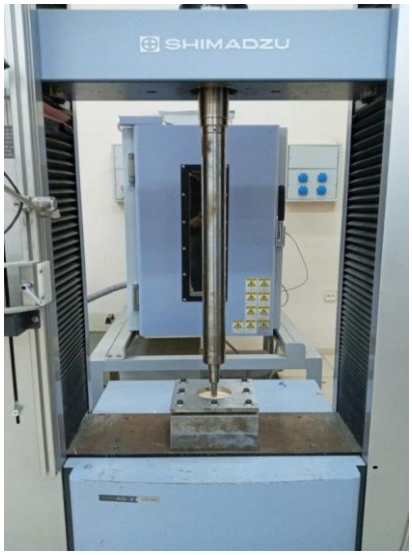


Figure 3.6 Test machine with punch-shear test apparatus (Personal archive, 2021)

3.3 Low Velocity Impact Test

Low velocity impact occurs during maintenance and service activities and is one of the most dangerous loads on the sheets of composite materials. (Mathivanan et al., 2010). There are many factors affecting the damage modes of composites in the low velocity impact event. These are fiber orientation, resin, material thickness, impact rate and tip type. (Ghasemnejad et al., 2010).

While metals can absorb energy in elastic and plastic deformation zones, composite materials can absorb energy in cases of damage and elastic deformation zones due to their fragile structure (Safri et al., 2014).

Low velocity impact damage in sandwich composites occurs as follows: The surface layer on the side where the tip hits is exposed to the reverse shear force. When the surface layer resists intrusion, extensive damage occurs in the surface layer. Separation occurs on the adhesion surface due to the deformation between the core and the surface layer. If the impact energy increases, the surface layer is pierced and reaches the end core and the core cells are separated from the fracture surface layers and shear damage occurs. If the draft side of the surface layer is loaded by the end, it will cause the lower surface layer to bend. Impact damage modes in sandwich

composites depend on the nose type of the impact device, the properties of the sandwich materials and the panel support conditions. If the surface layers are thin, the deflection is quite wide and the material draft is in damage mode. When the surface layer is thick, the deflection is very small and the material operates in the cutting damage mode (Abrate, 2011).

CEAST Fractovis Plus device was used in the impact test. The maximum energy output of the machine is 1800 Joules. It has a system that prevents rebound during the experiment that prevents the formation of repetitive impacts. The total falling mass of the impactor is 5 kg (included impactor and crosshead mass). The ends used are flat and hemispherical, with a diameter of 12.7 mm and a weight of 626 gr. With the data sensor connected to the striker tip, the data transferred from the striker tip is transmitted to the computer. Energy-time, force-time, force-displacement graphs are obtained with these data. In this study, energy levels of 80 J, 100 J and 120J were determined and tested with hemispherical, flat noses.

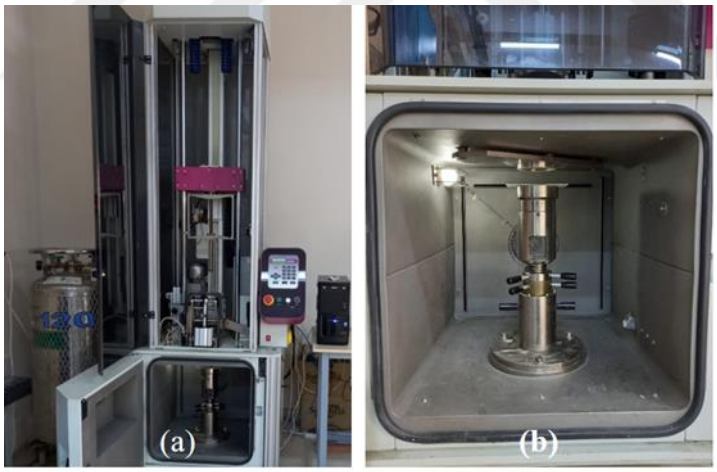


Figure 3.7 a) CEAST Fractovis Plus impact test machine, b) test chamber (Personal archive, 2021)

CHAPTER FOUR
RESULTS AND DISCUSSION

The mechanical properties to be sought in composite materials vary according to the place and conditions of the materials. The material type used in the study is sandwich composite consisting of PVC / S2 Glass. The low speed impact behavior of the composite material has been examined from different sides and the material has also been examined and discussed with the quasi-static punch shear test.

In this study, composite materials were produced in three different number of layers as 8, 10 and layers. The samples produced are obtained in the dimensions of 100 mm by 100 mm. Low speed impact test was applied to the cut samples by flat nose and hemispherical nose impactors with a diameter of 12.70 mm. Tests are conducted at three different energy levels and three repeats for each tests. Impact energies of 80J, 100J and 120J were selected for low speed impact tests. Force-time, energy-time and force-displacement a power-time diagrams were drawn according to the various impactoe velocites, number of ply and noses type. Maksimum contact forcea and absorbed energies are also obtained.

Punch Shear tests were conducted on samples by using Shimadzu AG-X 100 kN tension/compression test machine with flat nose and hemispherical nose penetrators of punch diameter of 12.70 mm. Tests are carried out for 1 mm/min, 5 mm/min, 15 mm/min, 25 mm/min and 50 mm/min of crosshead speeds. All tests are repeated three times. After the experiments, force-displacement diagrams were drawn according to the various crosshead speeds, number of ply and noses type. Maksimum contact forcea and absorbed energies are also obtained (Sarioglu et al., 2020).

The study will consist of three main sections as it depends on the different layer numbers, energy levels, nose types, speeds and test parameters of the samples used for this study.

- Impact Results
- Quasi-Static Punch Shear Results

4.1 Impact Results

At this stage of the research, composite samples to be used in experiments were determined. For this purpose, three different composites with different number of layers were produced and the change observed in the impact strength of these composites was investigated in two different nose types as flat nose and hemispherical nose.

4.1.1 Contact Force Results

In the contact force-displacement graphs, the priority of examination is given to the effect of the impact nose difference. Then, the effect of the number of layers was investigated. Figure 4.1 shows the force-time graphs of the 10-layer sandwich composite material subjected to 100 J impact loading with the hemispherical impact nose. As can be seen, the experimental results are very similar. In this study, the average values of this and other test group samples were taken while choosing graphics.

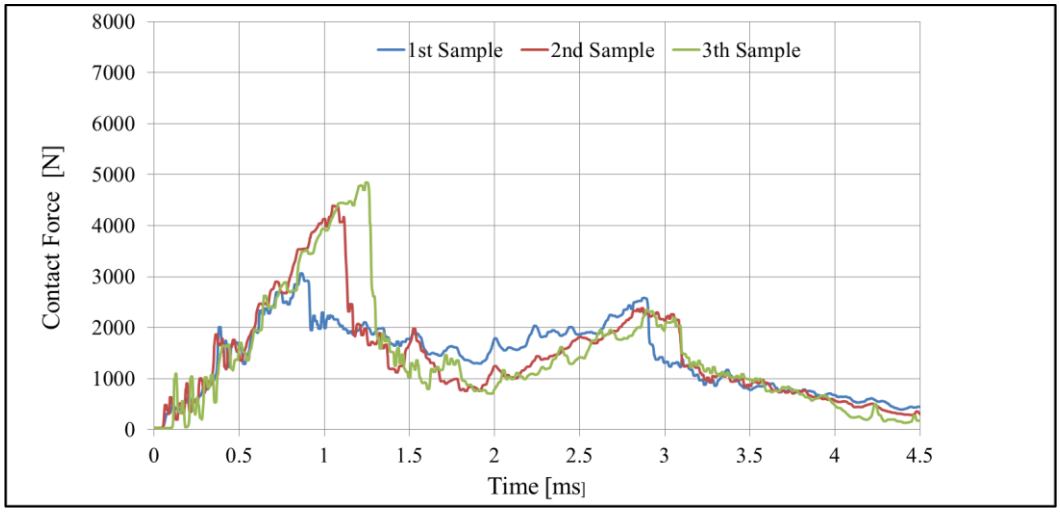


Figure 4.1 Force-time graphics of samples with 10-ply for hemispherical nose and 100J energy

Figure 4.2 shows the contact force-time diagrams with respect to impact energy for different impact noses and different layer numbers.

When the graphs are examined, a sudden drop occurs in the loading time profile after the damage begins. The reason for this is that the rigidity of the material is reduced. Damage matrix crack after this point, visible damage to the surface layer occurs. As the damage spreads, the load carrying capacity of the samples decreases. The second peak in the graph indicates that the material has been completely damaged. At this point, damage mechanisms such as fiber breakage and fiber delamination are seen. These damage combinations are mostly caused by penetration and perforation (Ude et al., 2013).

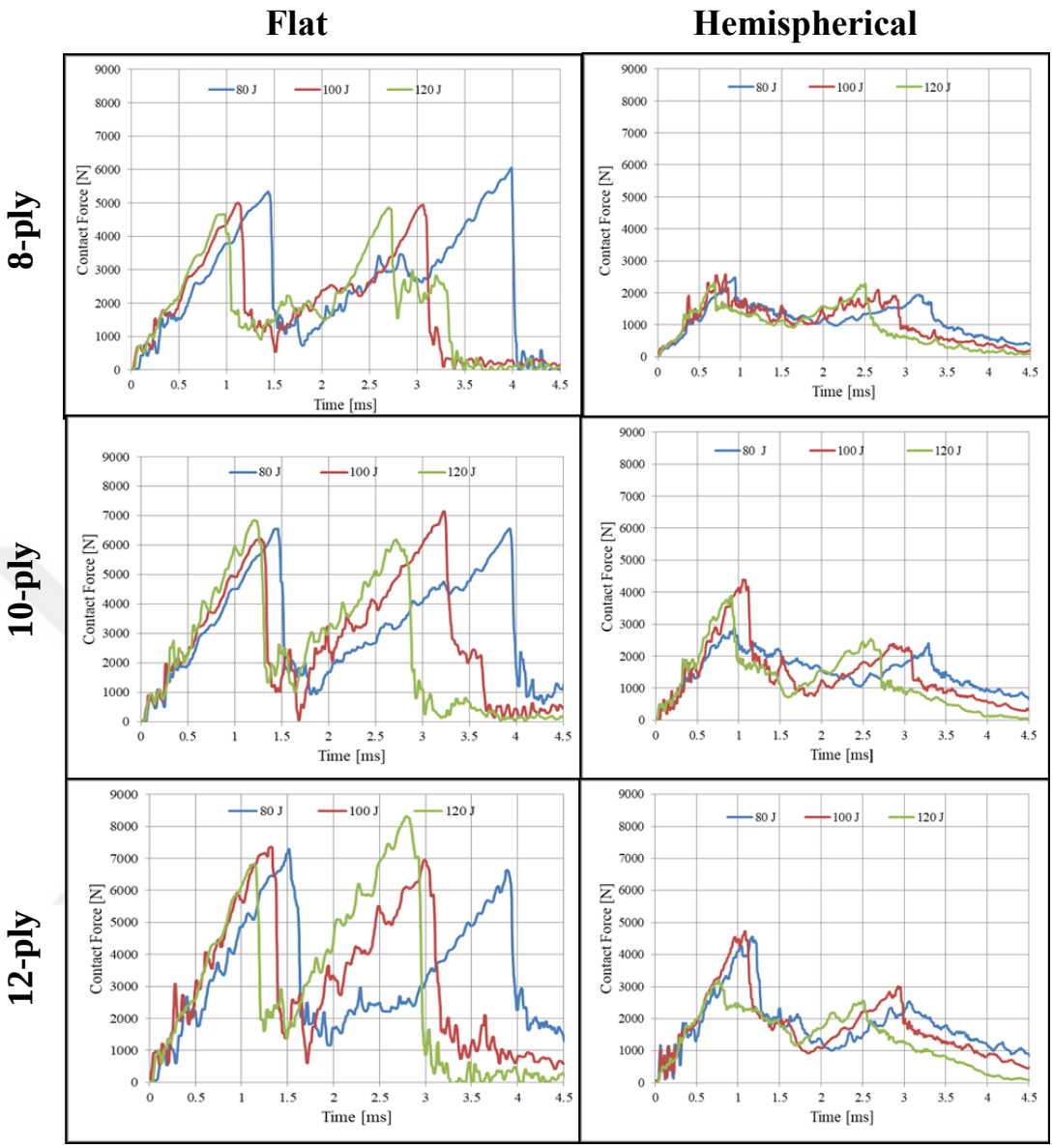


Figure 4.2 Contact force-time graphs according to the impact energy for different ply and impactor noses

When the graphs of the samples struck with a flat nose were examined, it shows that the fibers on the top surface of the first peak material were damaged. After the rise, a rise is seen again with a sharp fall.

This rise is the force generated by the compression of the foam between the sandwich materials. After the compressed foam is damaged, it makes a second peak

and after this peak there is a sudden drop in strength. The reason for this is an indication that the underlying fibers are damaged.

The sharp rise and fall in the graphics is due to the geometry of the impact nose. Tear damage was observed in the middle of the materials during experiments with the flat nose.

Damage modes such as puncture and penetration were observed in samples tested with a flat nose.

It has been observed that as the energy level decreases in the experimental samples, the contact force in the sandwich material increases. The reason for this is that the resistance of the material increases.

When the experiments with the hemispherical nose were examined, it was seen that the top surface layer of the first peak was broken. After a sudden drop, the foam between the materials is squeezed. The fall after the second peak indicates that the lower surface layer has been broken.

The peaks of the graphics in the experiments with the hemispherical nose appear to be more rounded. This is due to the geometry of the hemispherical nose. Damage modes such as puncture and penetration were observed in samples tested with a hemispherical nose. Hemispherical noses do not show tearing behavior to the material compared to flat noses; they show perforation behavior to the material.

It has been observed that the contact force decreases with the increase of the energy level at the hemispherical noses, as is the case with the flat noses.

Figure 4.3 gives the contact force-time graphs according to the number of layers for different impact energy and impact noses.

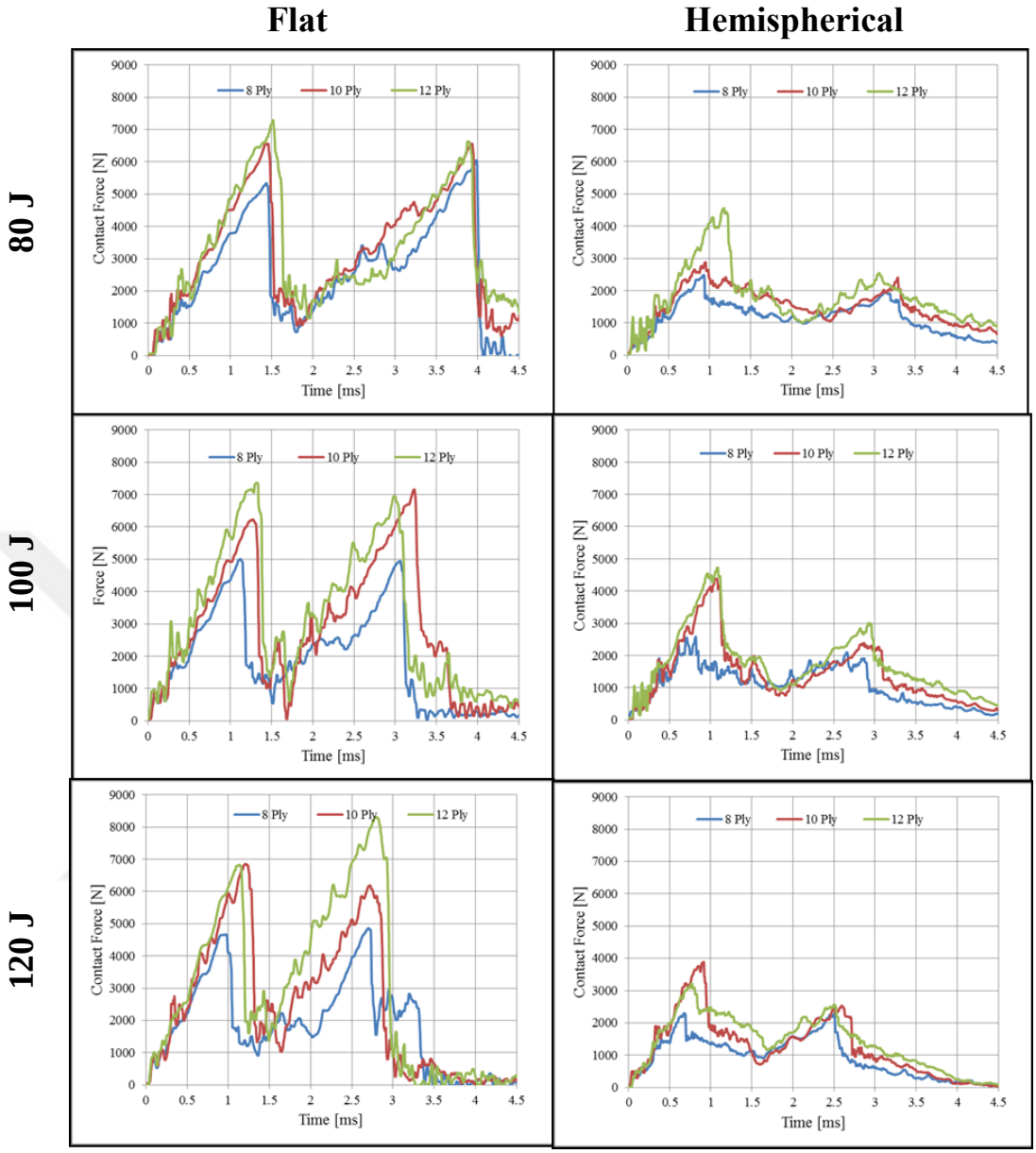


Figure 4.3 Contact force-time graphs according to the number of ply for different energy levels and impactor noses

When the flat section is examined in Figure 4.3, it was observed that the contact forces of the samples subjected to the experiment at the same energy levels increased with the increase in the number of layers. The first peak in the contact force of the 8-layer sample tested at 80 Joules was higher than the second peak.

It was observed that the difference between the first peak and the second peak in the contact forces of the 8-layer sample, which was tested at 100 Joules, decreased. It

is observed that the second peak in the contact force of the 8-layer sample subjected to 120 Joule test is higher than the first peak.

When the graphics tested with the hemispherical nose in Figure 4.3 are examined, it is seen that the contact force increases with the increase in the number of layers, such as the samples tested with the flat nose.

Similarly, it was observed here that the contact force in the upper surface layer decreased and the contact force in the lower surface layer increased with the increase of energy levels.

It can be concluded that the contact force decreases and the strength of the material increases with the increase in the energy level.

As the energy levels increase, the stiffness in the upper surface layer decreases and the rigidity in the lower surface layer increases (Balaban et al., 2019).

Energy levels of 80J, 100J and 120J were found to be perforation energy for each number of layers.

In the experiments, penetration energy level was not observed for each layer number and each nose type.

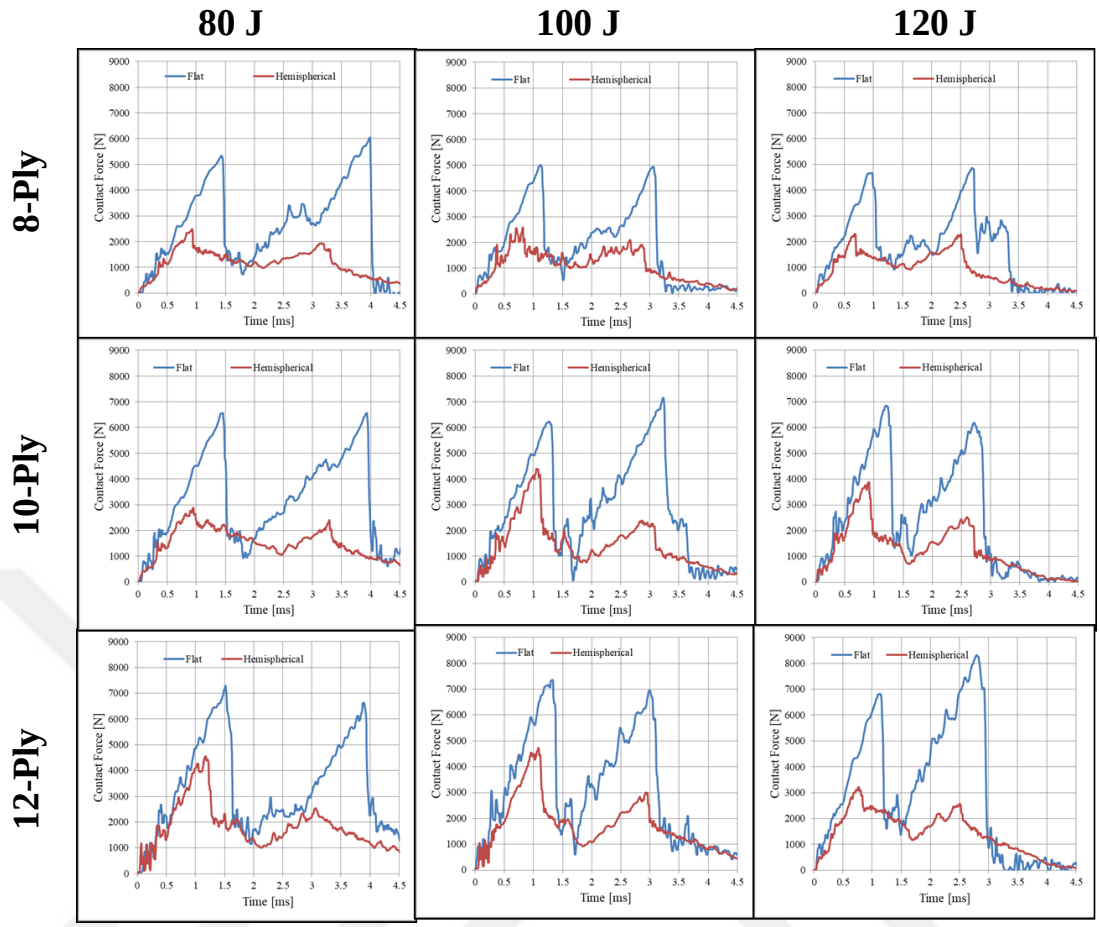


Figure 4.4 Contact force-time graphs according to impactor noses types for different energy levels and number of ply

When Figure 4.4 is examined, it is seen that the maximum contact force increases in all graphic types in the tests performed with the flat plunger. This is because the corners of the flat noses are sharp and the cutting force it creates when it comes into contact with the material is greater than the hemispherical nose. The flat nose causes more fiber damage, while the hemispherical nose causes more delamination damage.

In the experiments of 8-layer sandwich composites with both hemispherical and flat noses, it is seen that the value of the first maximum contact force and the value of the second maximum contact force converge with the increase of energy.

Table 4.1 Low velocity impact test results for different number of layers, nose types and energies

Number of Ply	Energy Levels [J]	Max. Contact Force[N]				Absorbed Energy [J]	
		Hemispherical		Flat		Hemispherical	Flat
		1.Peak	2.Peak	1.Peak	2.Peak		
8-ply	80J	2477	1936	5334	6049	29.59	53.81
	100J	2576	2089	5003	4937	36.66	52.96
	120J	2296	2281	4665	4858	35.20	56.15
10-ply	80J	2874	2400	6559	6559	41.39	65.60
	100J	4388	2381	6224	7154	40.49	67.59
	120J	3883	2525	6851	6185	39.46	69.13
12-ply	80J	4555	2539	7287	6635	43.96	67.65
	100J	4725	3007	7364	6947	50.92	75.06
	120J	3211	2562	6828	8316	41.71	77.39

Table 4.1 shows the calculated average values of the samples subjected to the low velocity impact test at 8, 10 and 12 face sheets and impact energies of 80J, 100J and 120 J, respectively. When Table 4.1 is examined, it is seen that the maximum contact force decreases with the change of the impact nose type in the experimental groups at the same impact energy for samples with 8, 10 and 12 layers.

In Table 4.1, it is seen that the maximum contact force from the samples exposed to the test with the flat nose occurred in 12-layer composite materials and 120J and its value is 8316 N. The lowest contact force was seen at 120 J with 8 layers and its value was found to be 4858 N.

In Table 4.1, it is seen that the maximum contact force from the samples exposed to the test with the hemispherical nose occurred in 12-layer composite materials and 100J and its value is 4725 N. The lowest contact force was seen at 120 J with 8 layers and its value was found to be 2296 N.

Figure 4.5 shows contact force-velocity graphs according to the face sheets for different impact energy and impactor noses.

When Figure 4.5 is examined, the kinetic energy formula of the energy levels and the mass of the impact nose are known and the velocities of the 80J, 100J and 120J

impact energies are calculated. The velocity of the impact energies is obtained using equation (4.1).

$$E_k = \frac{1}{2} \times m \times v^2 \quad (4.1)$$

Where E_k, m and v are the kinetic energy, the mass and the velocity of the impactor just before contact with the composite. The mass of the impactor is 5.025 kg. When 80, 100 and 120 J impact energy (E_i) levels are written in equation 4.1 (E_i=E_k), their velocities are found as 5.62, 6.31, 6.91 m/s, respectively.

When the graphs of sandwich composites consisting of 8 surface layers are examined, it is observed that the maximum contact force decreases with the increase of velocity in the tests performed with flat noses. . This is because the highest contact force is seen at 5.64 m/s speed. However, in the samples tested with hemispherical noses, as the speed increases, the first peak contact force decreases, while the second peak contact force increases.

When the graphs of sandwich composites consisting of 10 surface layers are examined, it is seen that the first peak maximum contact force decreases and the second peak maximum contact force increases as the speed increases in the samples tested with flat nose. The highest maximum contact force at the first peak is seen at 6.91 m/s velocity, while the highest maximum contact force value at the second peak is seen at 6.31 m/s velocity. In the samples tested with the hemispherical nose, the highest contact force at the first peak is observed at the velocity value of 6.31 m/s. The highest contact force value at the second peak is seen at 6.91 m/s velocity.

When the graphs of sandwich composites consisting of 12 surface layers are examined, it is seen that the first peak maximum contact force decreases while the second peak maximum contact force increases with the increase in speed for the flat nose. However, in the samples tested with the hemispherical nose, it is seen that both the first peak and the second peak contact force decrease as the speed increases.

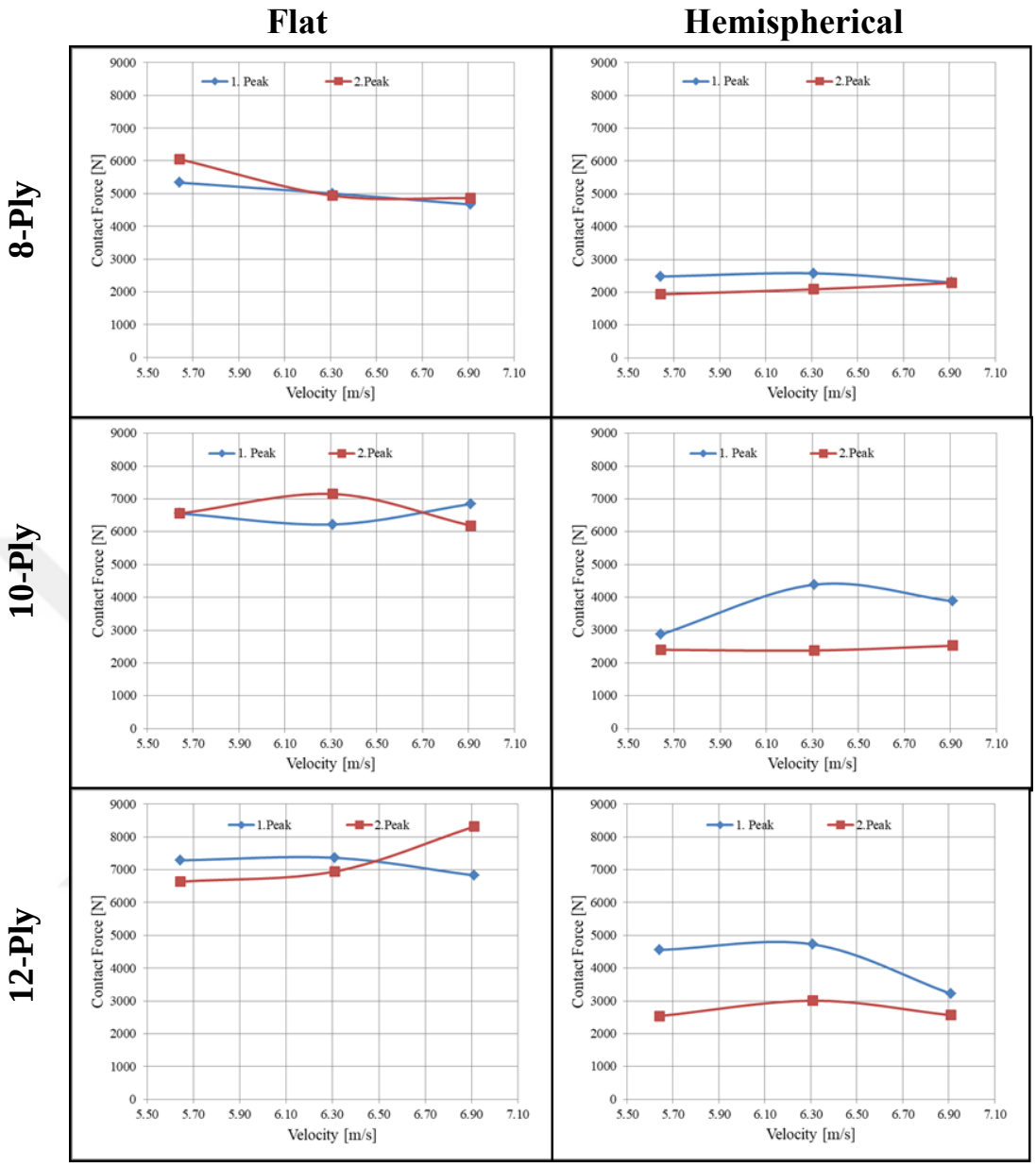


Figure 4.5 Contact force-velocity graphs according to the number of ply for energy levels and impactor noses

4.1.2 Absorbed Energy

Energy-time graphs are examined in two parts. It is thought that the energy absorbed up to the first part peak load is absorbed in the elastic region for sandwich composites, and the part after the peak load is absorbed by the damage caused by the energies in the material. The amount of energy absorbed in sandwich materials is

obtained by the sum of the energy absorbed in the elastic zone and the amount of energy absorbed beyond the elastic zone. If the impact energy penetrates the material, the amount of energy absorbed decreases and the damage becomes localized (Ude et al., 2013).

Figure 4.6 shows definition of impact energy, absorbed energy on energy-time graph of impact test.

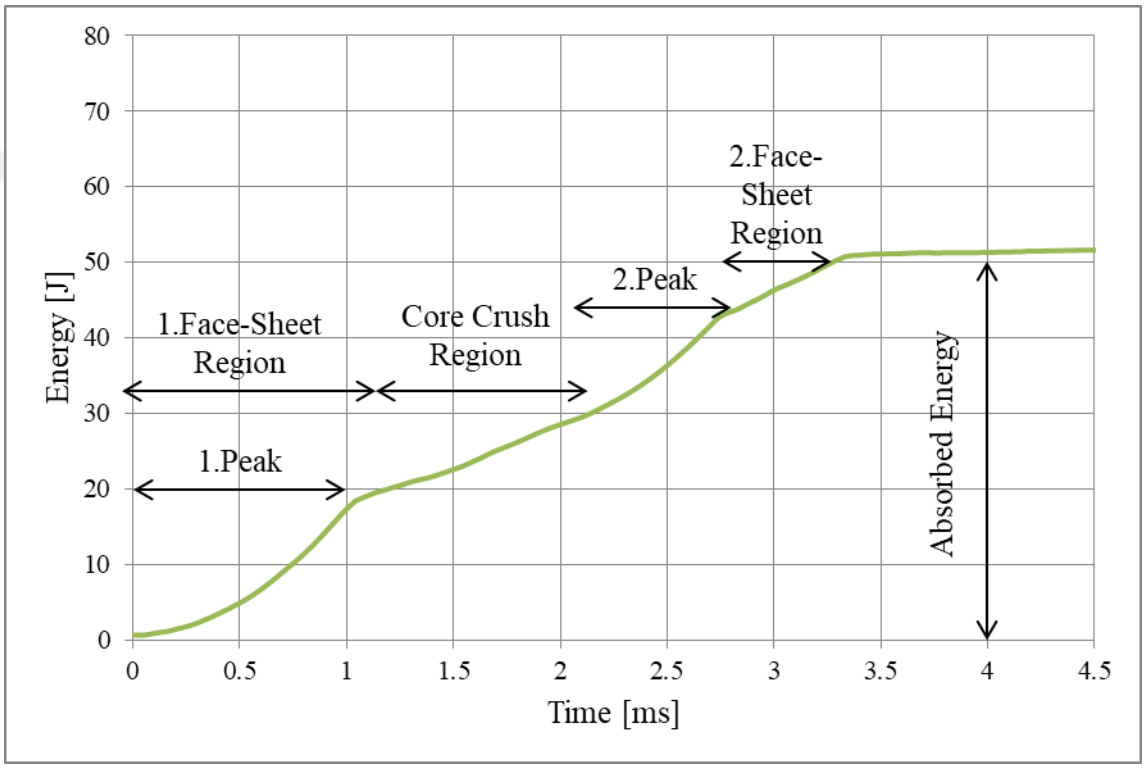


Figure 4.6 Definition of the impact energy of the 8-layer sandwich composite tested with a flat nose and 120J energy, energy absorbed in the energy-time graph

Figure 4.6 shows the energy-time changes of sandwich composites depending on the energy.

When Figure 4.7 is examined, samples that have been tested with a flat nose are seen with initial penetration energy of 80J. Not all of the impact energies were absorbed for all three layer numbers and the tested energy levels were not reached.

When the graphics are examined, it shows the strength of the first peak top surface layer. Then the decreasing increase of the graphic indicates that the upper surface layer is damaged. The third rising part shows the compression of the foam. The last part indicates the strength of the lower surface layer and the following flatness indicates that the material is pierce

When examining the samples tested in 3 different layer numbers and at the same energy levels with the flat nose, it is seen that the absorbed energy increases when the number of layers increases.

When the graph with 8-layer samples is examined, it is seen that the sample tested at 80J energy level absorbs the most energy. However, with the increase in the number of layers, the highest energy absorbing energy level appears to be 120J.

When the graph with 10-layer samples is examined, it is seen that the difference between the amount of energy absorbed by the samples tested at 80, 100 and 120J energy levels is small.

It is observed that the amount of energy absorbed by the samples tested with the hemispherical nose increases with the increase in the number of layers.

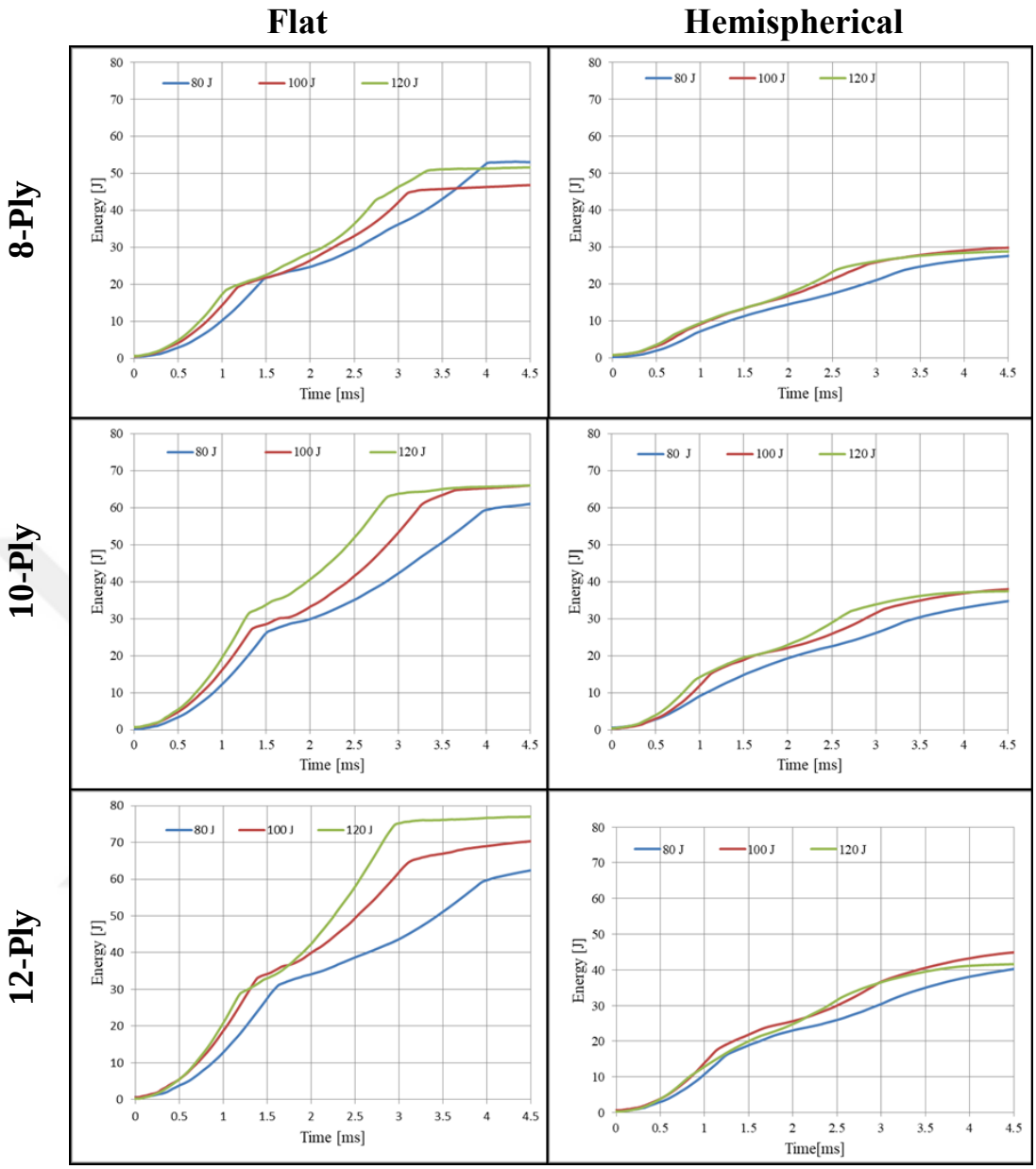


Figure 4.7 Energy-time graphs depending on energy change

Figure 4.8 shows the energy-time changes depending on the number of layers.

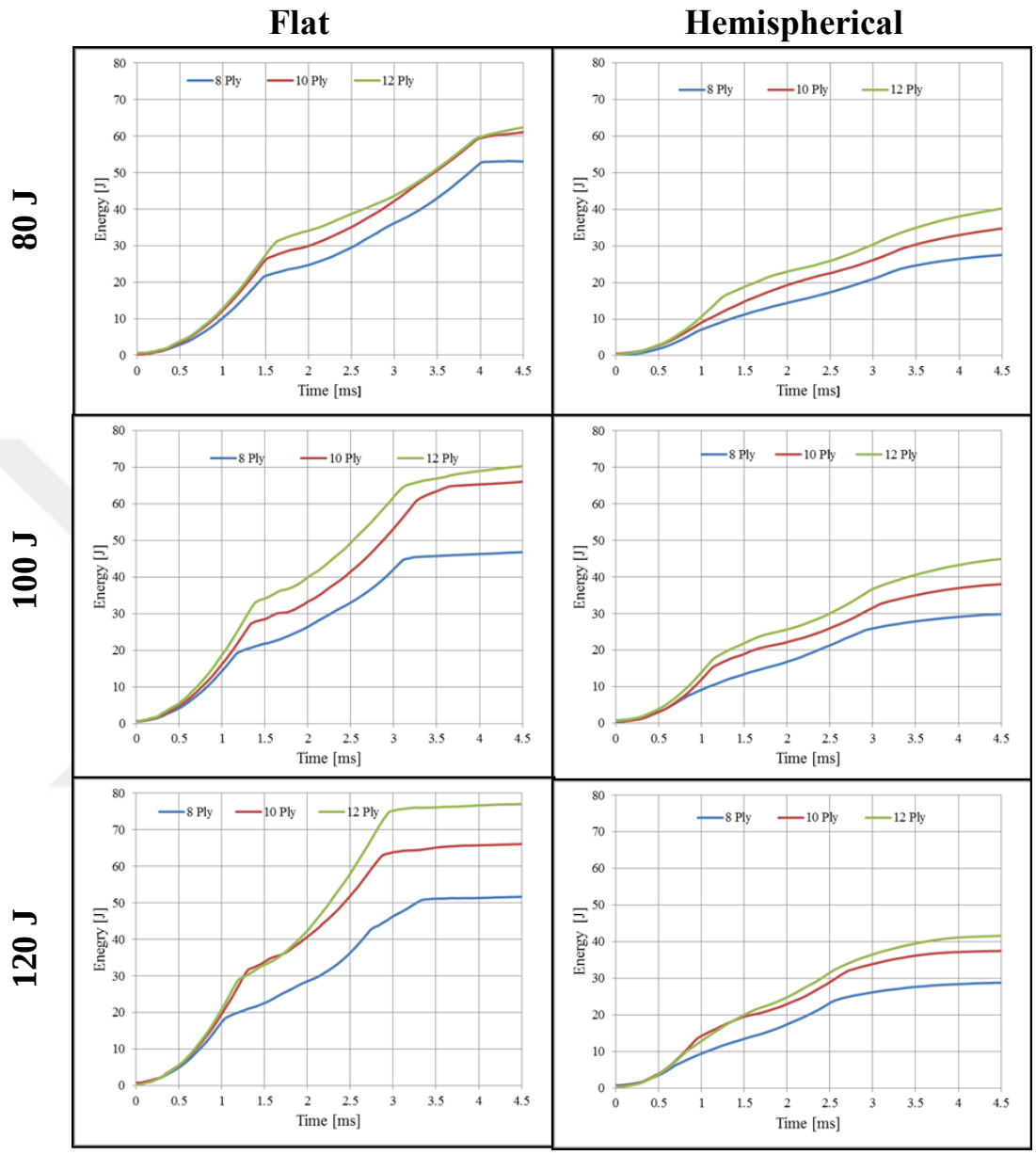


Figure 4.8 Energy-time graphs due to number of ply

When the graphs in Figure 4.8 are examined, the absorbed energy increases due to the increase in the number of layers in samples tested with flat noses for 80J. The increasing and decreasing part of the graph lasted for the shortest 8-layer samples.

It is seen that the crushed absorption energy value of the foam is the highest in the 12-layer composite sample.

It has also been observed that the parabolic curves in foam crushing converge at certain intervals of second.

When the graphs at 100 J are examined, it is seen that the increase in the number of layers and the increases in the absorbed energy are sharply separated.

When the graphs at 100 J are examined, it is seen that the increase in the number of layers and the increases in the absorbed energy are sharply separated.

When the graphs at 120 J are examined, the decreasing and increasing part of the graph converges for the 10 and 12 layers, and it is proven here that the amount of energy absorbed by the higher number of layers is high with the separation of the graphics in foam crushing.

In the samples tested with the hemispherical nose, when the graphs at 80 J and 100 J are examined, it is seen that the amount of energy absorbed increases with the increase in the number of layers. Although it rises close to each other in the first peaks of the graphs, it is seen that the second rising part and the parts absorbed by the foam are separated from each other. On the graphs at 120 J, it is seen that the first peak and the decreasing and increasing parts of the 10 and 12 layers are separated by the amount of energy absorbed by the foam crushing.

Figure 4.9 graphically shows the energy-time changes of impact noses tested on materials. When Figure 4.9 is examined, it is observed that the amount of energy absorbed by the samples tested with the flat nose is more than the amount of energy absorbed by the samples tested with the hemispherical nose. While the graphics of samples tested with flat noses show a sharper rise, samples tested with the hemispherical noses rise blunt.

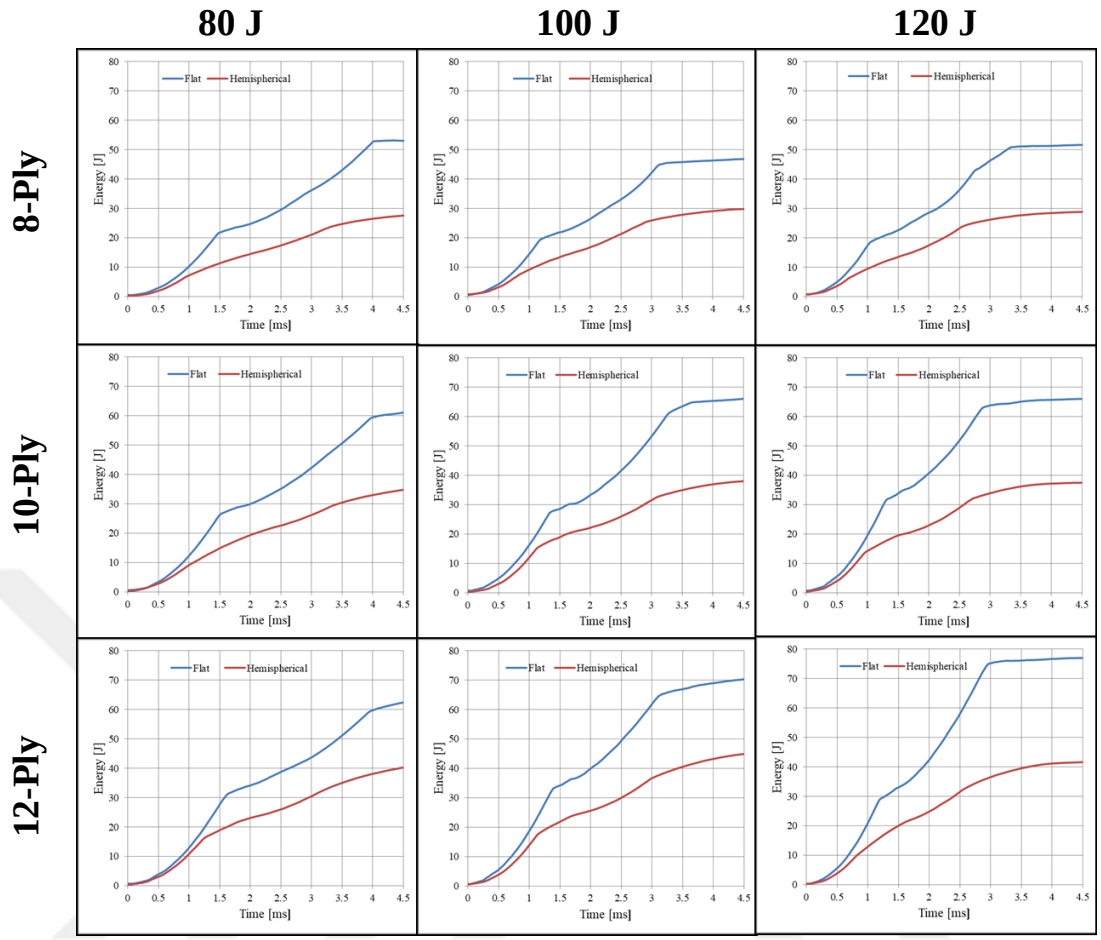


Figure 4.9 Energy-time graphs due to impactor noses

Figure 4.11 shows power-time graphs according to the energy levels for different face sheets and impactor noses. The power of the impact energies is obtained using equation (4.2).

$$\frac{dE}{dt} = P \tag{4.2}$$

E is the energy absorbed by composite at any time and P is the power applied to the composite by the impactor.

Table 4.2 Composite applied power results for different number of layers, nose types and energies

Number of Ply	Energy Levels [J]	Power[W]			
		Hemispherical		Flat	
		1.Peak	2.Peak	1.Peak	2.Peak
8-ply	80J	13.6	9.48	26.4	20.7
	100J	16.0	11.9	29.4	24.3
	120J	16	14.7	31.2	28.5
10-ply	80J	15.6	12.7	31.4	19.7
	100J	26.5	12.9	35.1	30.1
	120J	26.3	15.8	43.1	32.3
12-ply	80J	23.5	11.4	33.5	19.9
	100J	27.8	15.5	39.4	28.3
	120J	22.2	15.8	43.7	40.1

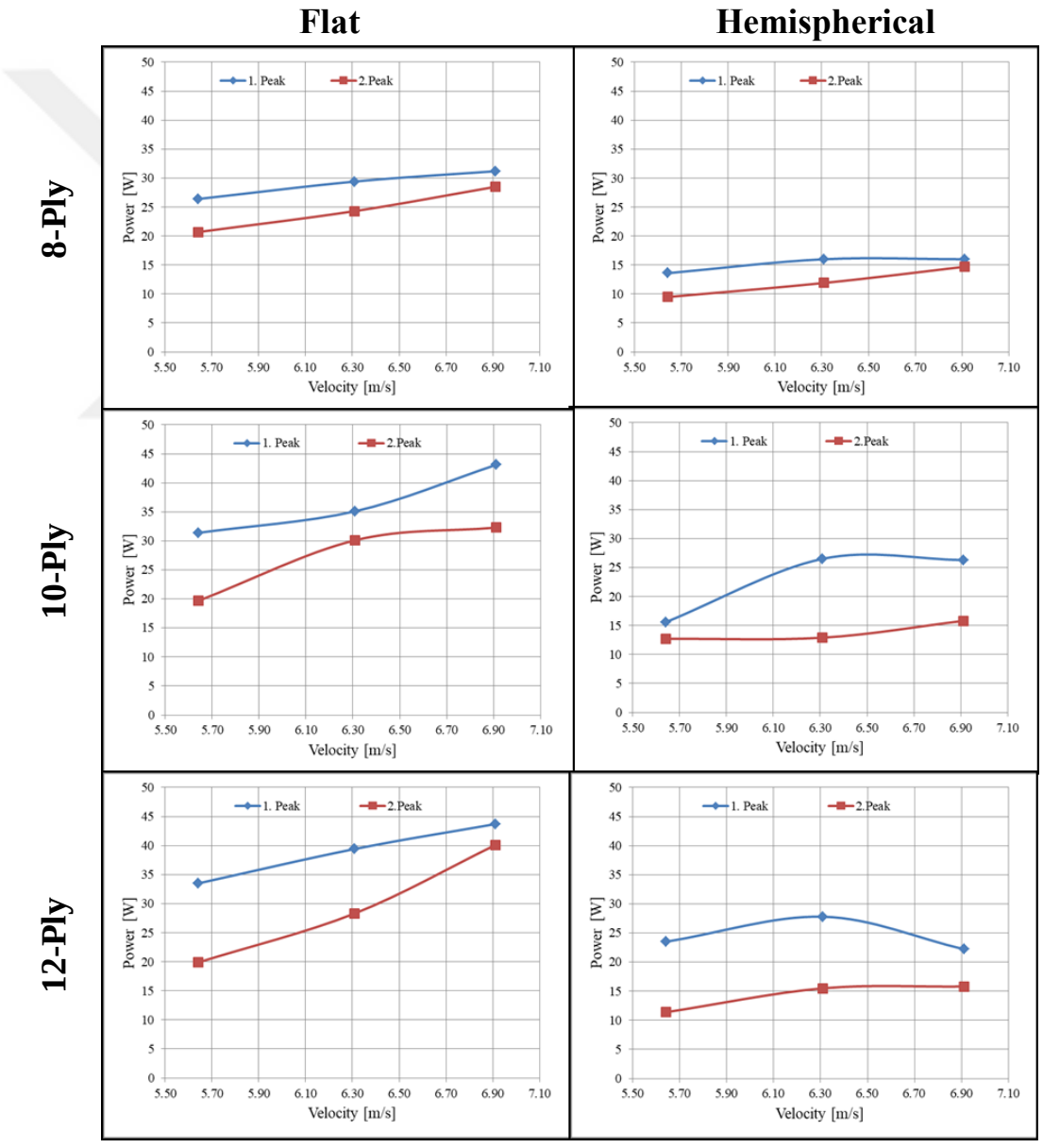


Figure 4.10 Power-velocity graphs according to number of ply and impactor noses

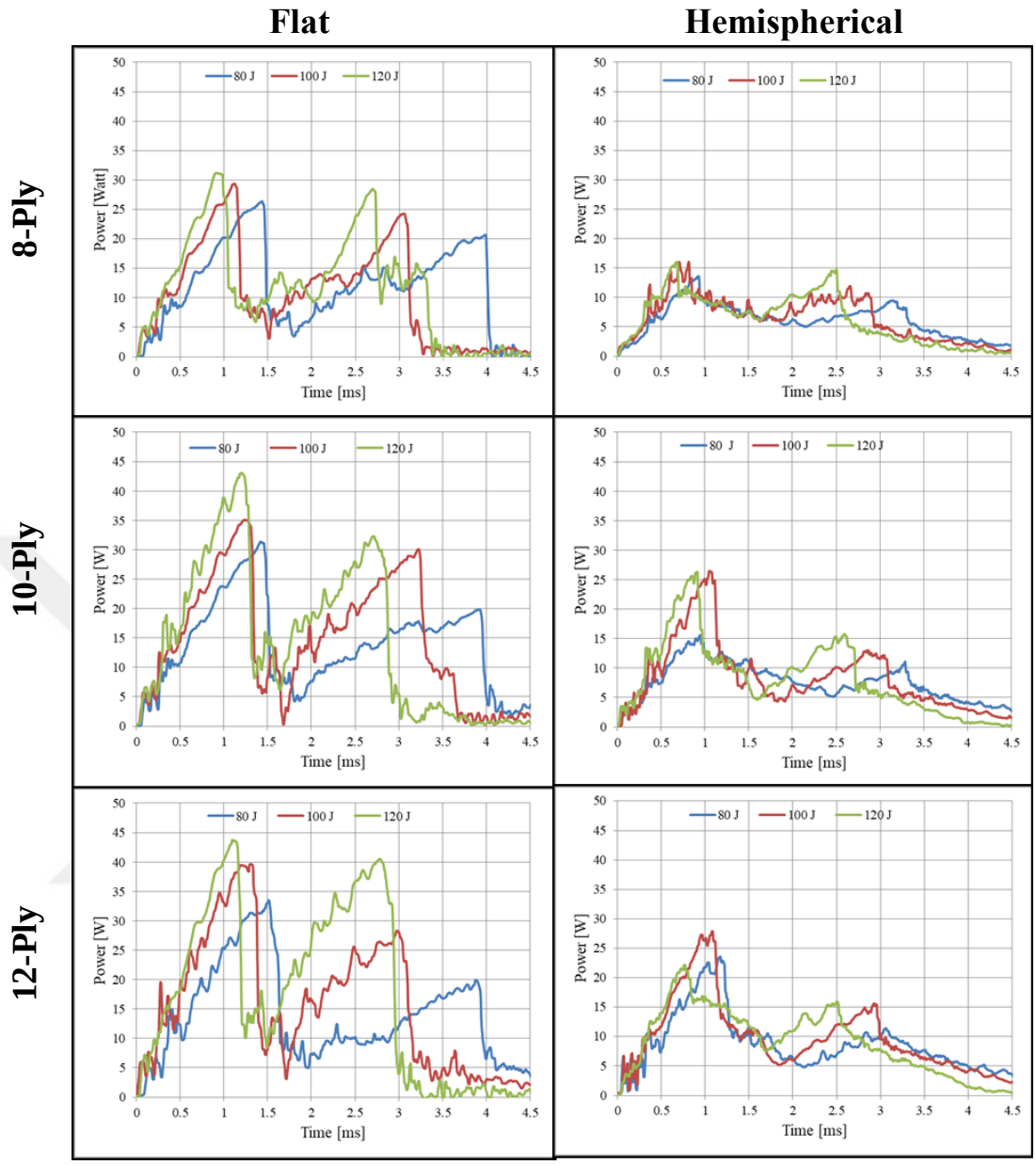


Figure 4.11 Power-time graphs depending on energy change

When the graphs of the samples tested with the flat nose are examined, it is seen that the power increases as the energy level increases. It is seen that the power increases with the increase in the energy level in the samples tested with the hemispherical nose.

Figure 4.12 shows power-time graphs according to the number of layers for different energy levels and impactor noses.

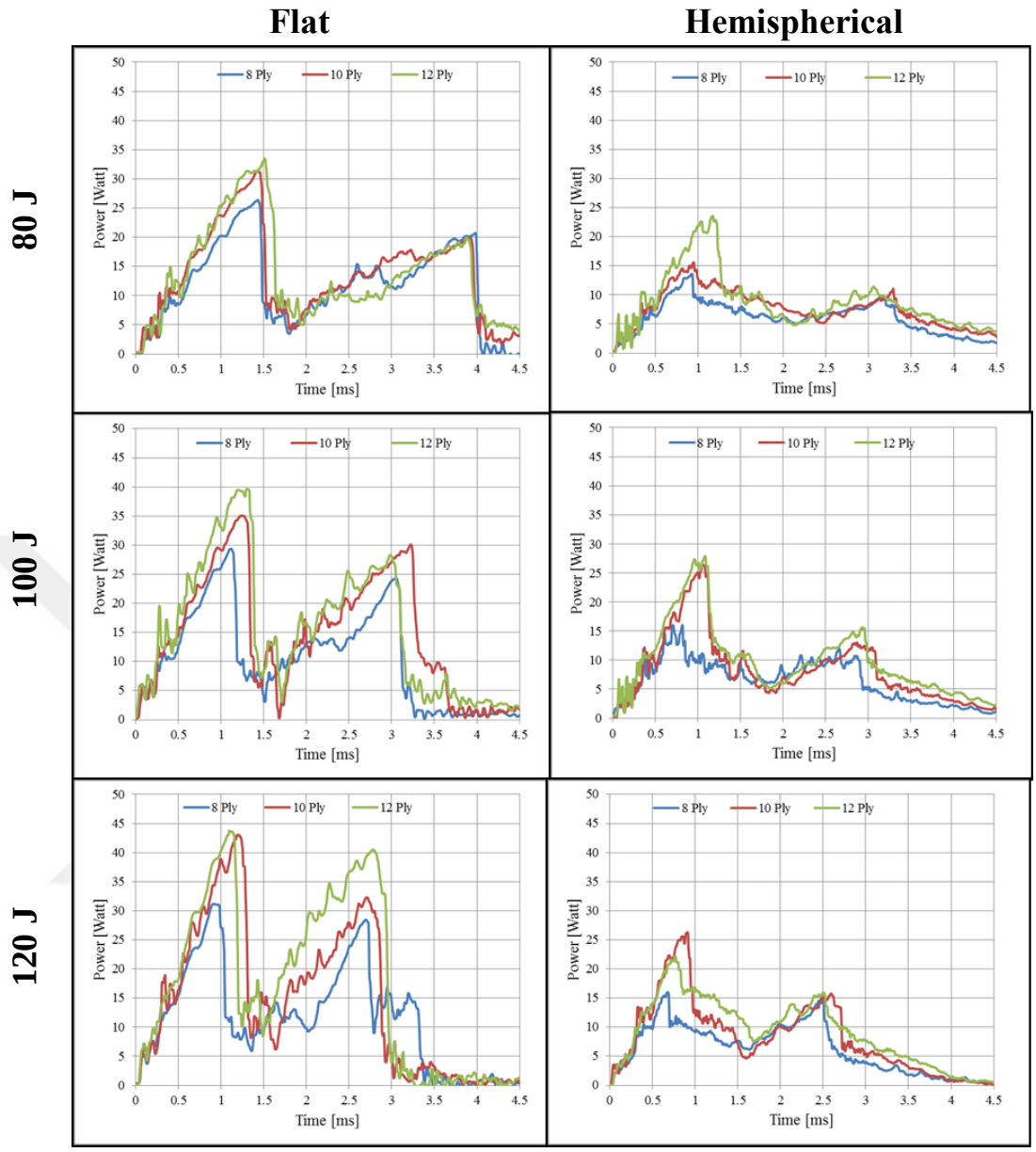


Figure 4.12 Power-time graphs due to number of ply

When the samples subjected to the test with a flat nose are examined, the increase in the number of layers indicates an increase in the amount of power it creates in the material.

In the samples tested with the hemispherical nose, it is seen that the 12 layer samples are hit with the highest power at the 80J energy level, while it is seen that the power amount of the 12 layer samples is less than the power amount of the 10 layer samples when the energy levels are increased.

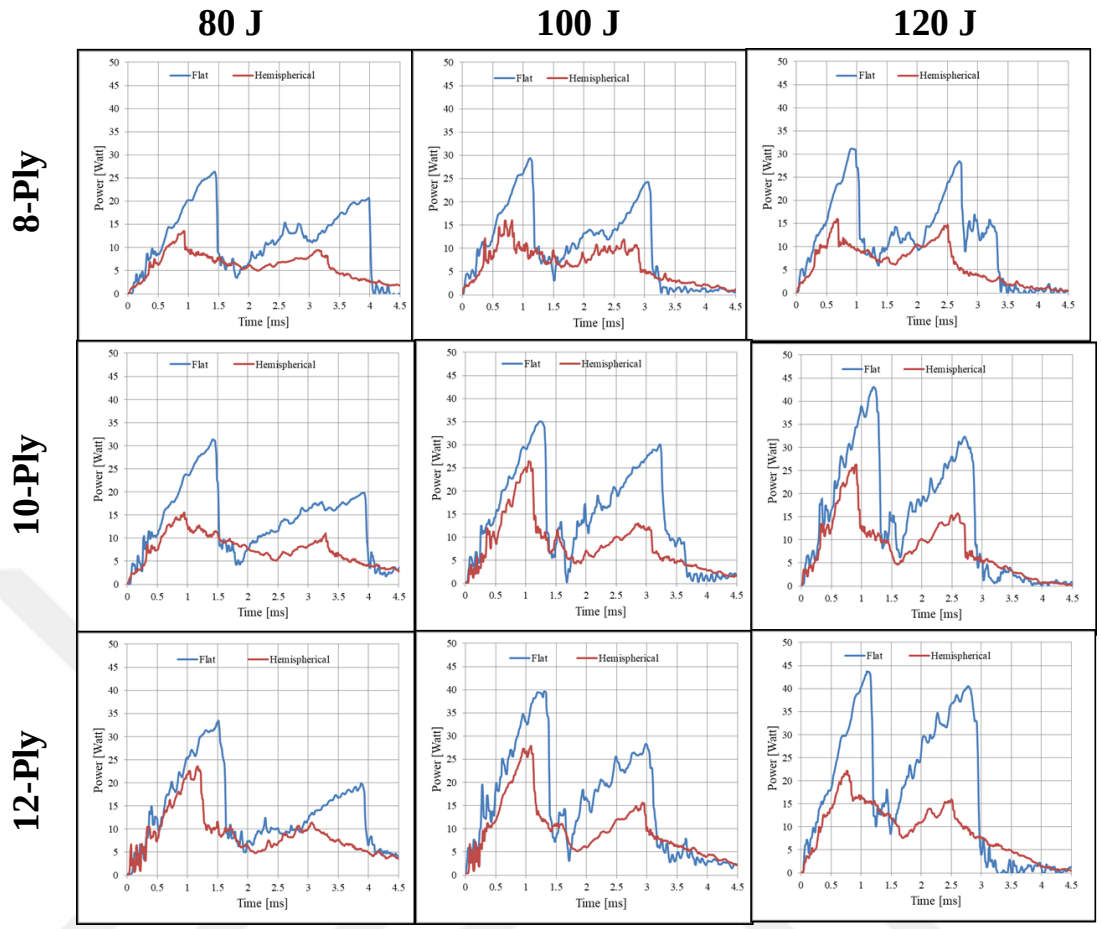


Figure 4.13 Power-time graphs due to impactor noses

Figure 4.13 graphically shows the power-time changes of the impact noses tested on the materials. When Figure 4.12 is examined, it is seen that the applied power of the samples tested with the flat nose is more than the applied force of the samples tested with the hemispherical nose

4.1.3 Impact Damage

In this section, damages on the specimen after low velocity impact tests were examined by visual inspection. Damages to the front and back surfaces of the samples tested have been examined for 8, 10 and 12 layers, respectively as shown in in Figure 4.14, Figure 4.15 and Figure 4.16 according to the three different layer numbers, two different type noses as flat and hemispherical nose and energy values of 80J, 100J and 120J.

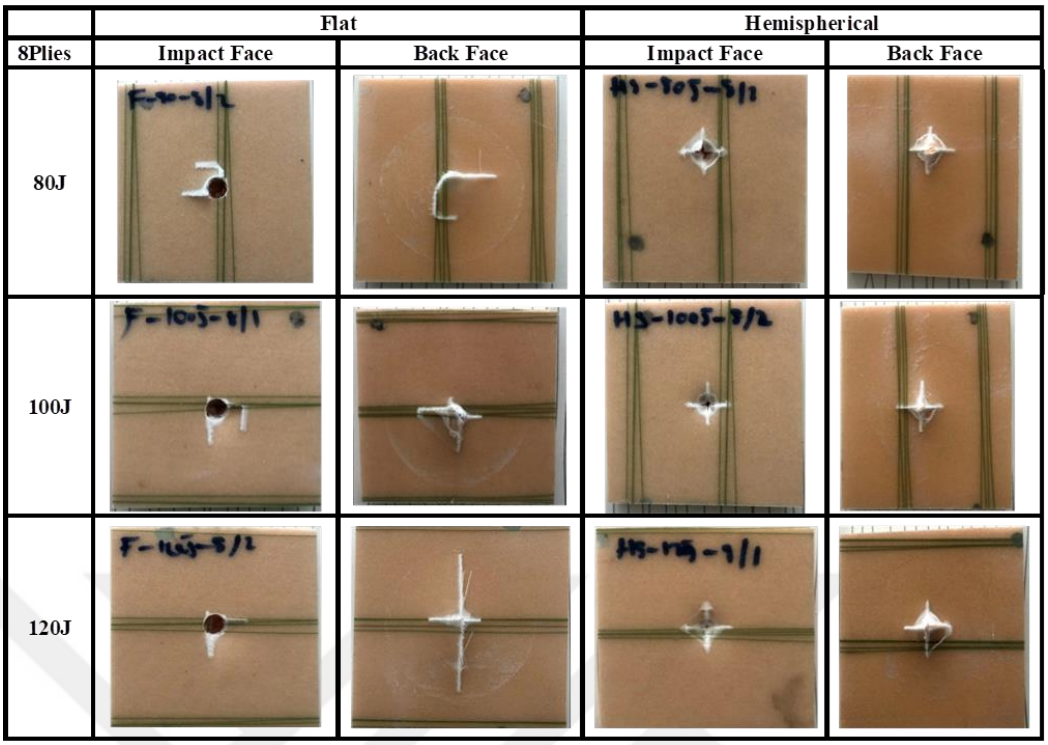


Figure 4.14 Impact damages types of sandwich composite samples with flat and hemispherical noses at different impact energies at 8 ply

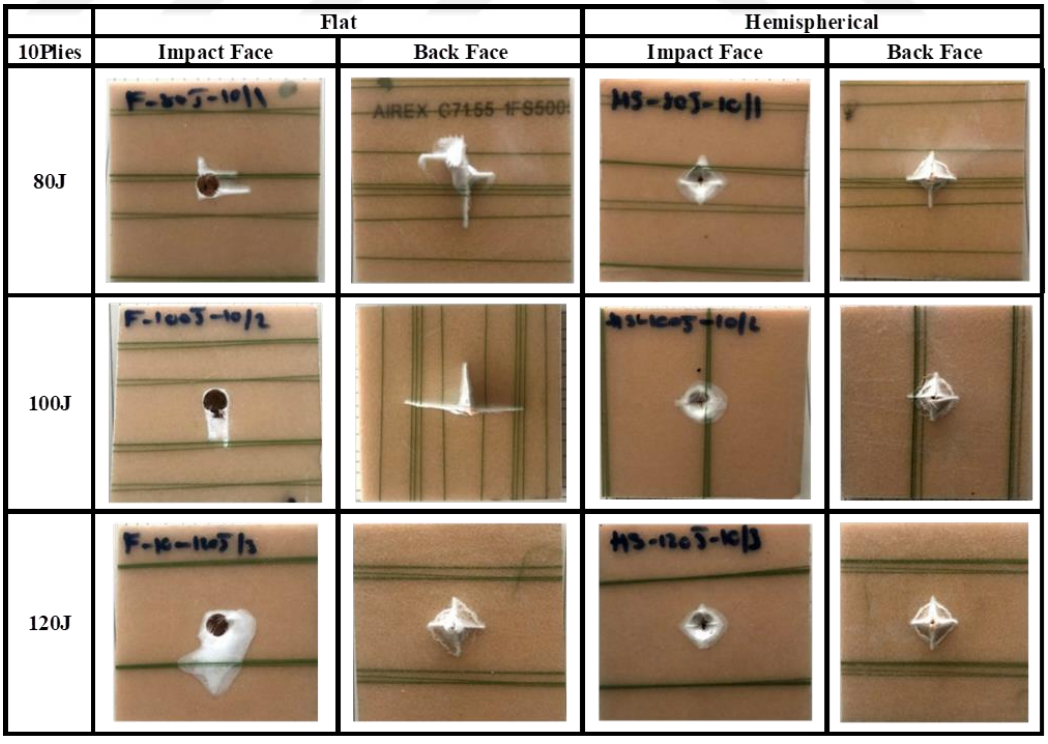


Figure 4.15 Impact damages types of sandwich composite samples with flat and hemispherical noses at different impact energies at 10 ply

When Figure 4.13, Figure 4.14, Figure 4.15 are examined, it is seen that the materials are subject to puncture for both nose types and each number of layers. The samples at the energy levels subjected to the test suffered fiber and core damage.

When examined as nose types, it is seen that the flat nose type forced the rear surface to tear. Looking at their upper surface, a sharper puncture is seen due to the sharp corners of the nose.

Looking at specimens tested with the hemispherical nose, there is a smoother puncture damage due to the blunt parts around the nose.

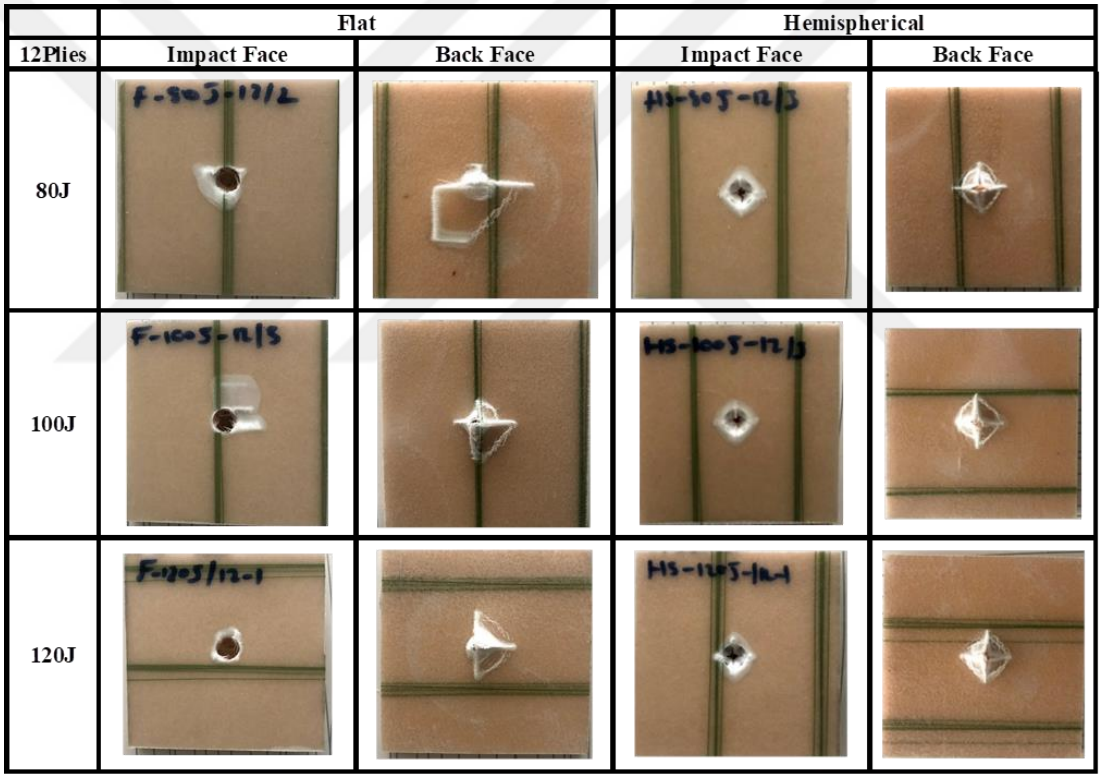


Figure 4.16 Impact damages types of sandwich composite samples with flat and hemispherical noses at different impact energies at 12 ply

When the back face of the samples tested with the flat nose is examined, debonding is observed between the back surface layer and the core. When the damages on the upper surfaces are examined, delamination, fiber separation and bending damages are generally observed.

4.2 Quasi Static Test Results

In this section, the results of quasi-static tests for penetration and perforation conditions of materials were examined. It will be possible to understand this situation by force-displacement and energy-time graphs.

The purpose of the quasi-static punch shear test is to examine the behavior of the low speed impact test on the material, because it is an easier method to calculate the absorbed energy.

Sandwich composites consisting of 8 layers, 10 layers and 12 layers were subjected to low velocity impact tests with energy levels of 80 J, 100 J and 120 J and with two different nose types, hemispherical, flat nose. Subsequently, samples with the same number of layers and nose types were subjected to quasi-static punch shear test at 5 different speeds: 1 mm/min, 5 mm/min, 15 mm/min, 25mm/min and 50 mm/min.

Quasi-static test results were averaged by performing at least three repetitions for each experimental group. Figure 4.16 shows the quasi-static test results of the samples subjected to the test at five different speeds with hemispherical noses for 10-layer sandwich composite.

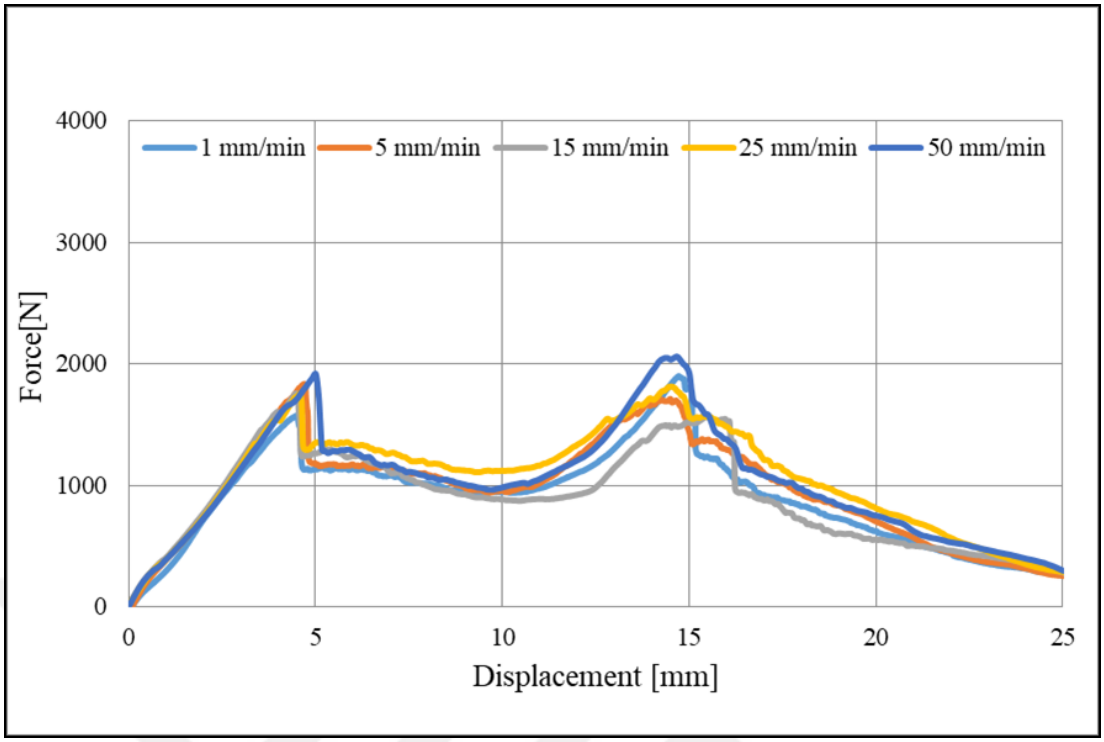


Figure 4.17 Quasi-static test results of samples with 10layer subjected to hemispherical nose and 5different speeds

4.2.1 Force-Displacement Results

Maximum forces and absorbed energies are given in Table 4.2.

When Table 4.2 is examined, it is seen that the maximum force decreases and the absorbed energy increases with the increase of speed in the samples tested with flat and hemispherical noses. In addition, the increase in the maximum strength is observed with the increase in the number of layers.

Table 4.3 Maximum forces and absorbed energies of quasi-static test for 8 ply, 10 ply and 12 ply specimens at different speeds and noses

Number Of Ply	Speed [mm/min]	Max Force[N]				Energy[J]	
		Flat		Hemispherical		Flat	Hemispherical
		1.Peak	2.Peak	1.Peak	2.Peak		
8 Ply	1	2147	2586	1227	1363	23.64	17.38
	5	2562	3060	1493	1984	24.80	20.09
	15	2549	2957	1462	1447	31.06	19.18
	25	2619	3514	1413	1492	32.24	19.25
	50	2611	3441	1413	1329	29.09	20.10
10 Ply	1	2780	3309	1579	1901	29.17	23.14
	5	2874	3530	1295	1837	26.13	22.61
	15	3126	3821	1760	1548	28.35	20.40
	25	2992	3816	1756	1815	31.27	24.77
	50	3211	3517	1918	2062	26.57	25.66
12 Ply	1	3084	3939	1902	1829	33.13	24.83
	5	3326	4239	2249	2011	36.90	26.40
	15	3369	3724	2245	1623	33.39	26.42
	25	3303	4975	2202	1849	42.26	26.29
	50	3468	4487	2269	2092	42.30	28.00

Quasi-static test force-displacement graphs were drawn as shown in Figure 4.18.

When the graphs in Figure 4.17 are examined, it is seen that the graphs with quasi-static test are compared according to five different speeds.

When the samples tested with flat noses are examined, it is seen that the maximum force value decreases with the increase of speed. When the graphics are examined section by section, the strength of the upper surface layer with the loading is shown in the first rise. Then the first sudden drop in the graph indicates that the top surface layer has been damaged. The area between the first surface layer and the second elevation of the graph shows that the core material between the sandwich materials is compressed due to loading. The second rising part of the graph indicates that the substrate layer has begun to be damaged, and the sudden drop of the graph here indicates that the substrate layer has been damaged.

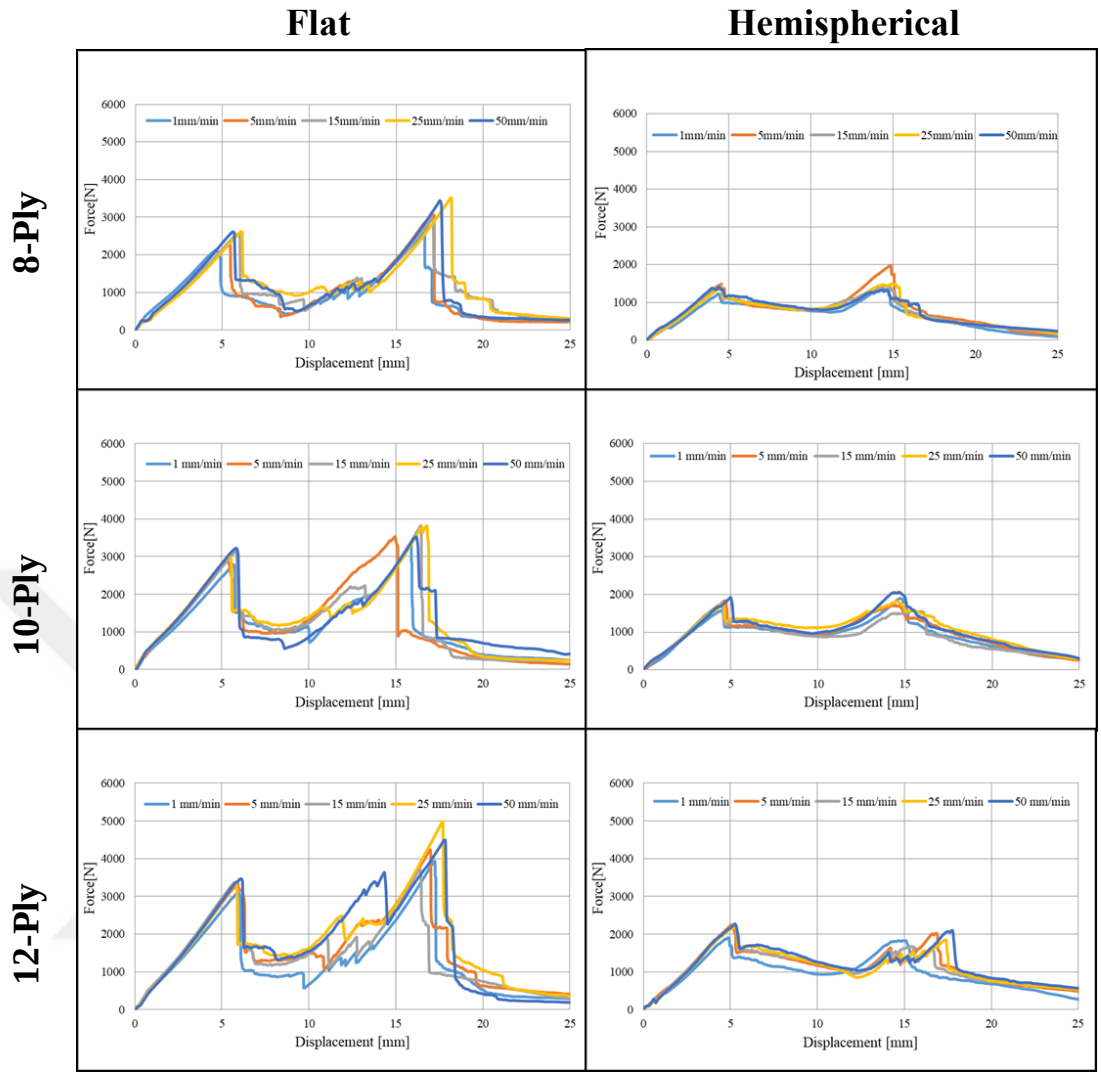


Figure 4.18 Force-Displacement graphs according to the various crosshead speeds for different ply and noses

When the graphs of the samples tested with the hemispherical nose are examined, it is seen that the sharpness of the loading drop in the first surface layer damages is less, although the first rising parts of the graphs are the same as the flat nose. The foam jam portion appears to be similar to that tested with the flat nose. The onset and damage of the substrate layer on the graph is less sharp than that of the flat nose.

When the graphs in Figure 4.19 are examined, it is seen that the graphs with semi-static tests are compared according to the number of three different layers.

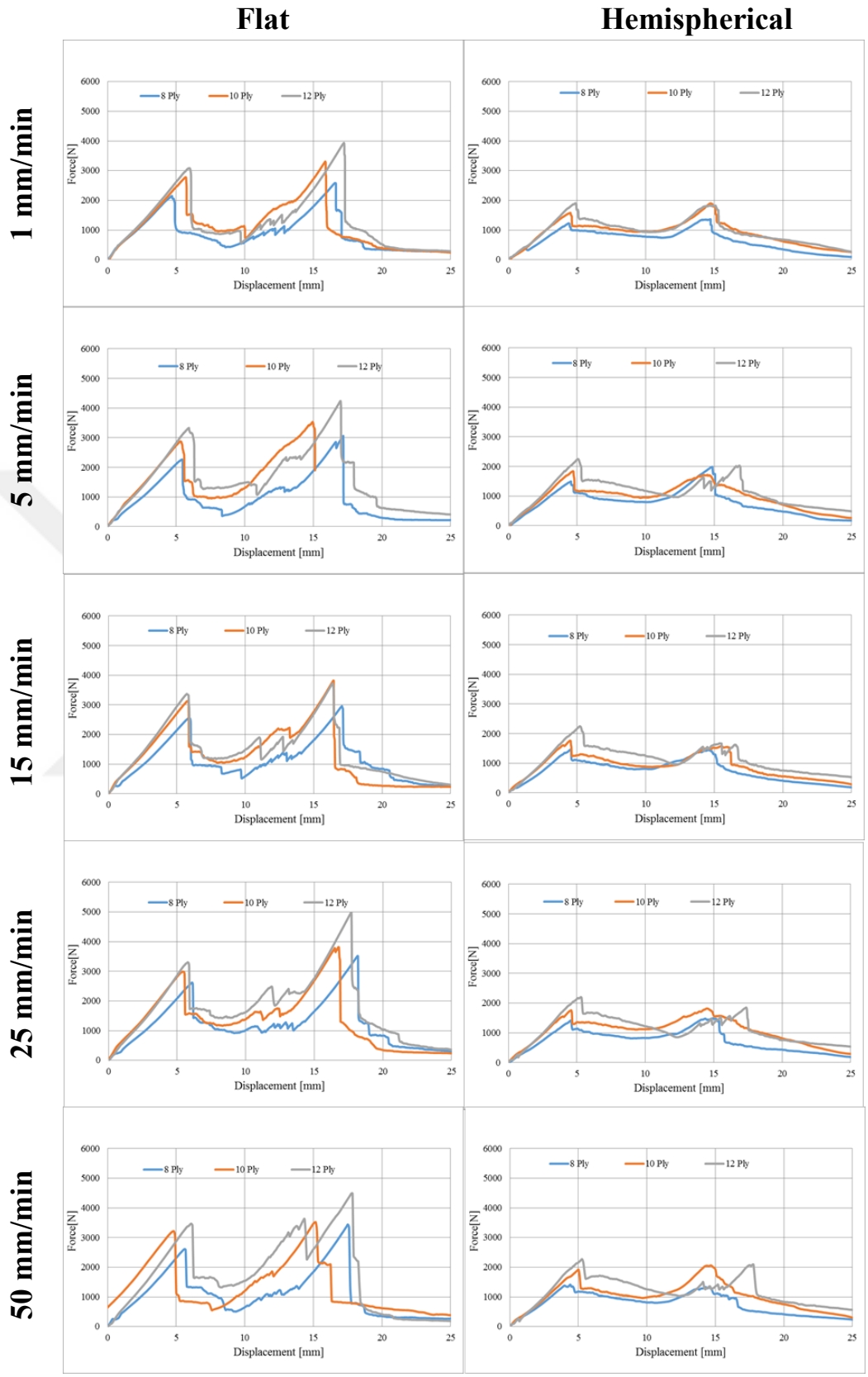


Figure 4.19 Force-displacement graphs according to the number of ply for different crosshead speeds and noses

When the samples tested with the flat nose are examined, it is seen that the strength increases with the increase in the number of layers. In the samples tested at 25 mm/min, the number of layers of 12 appears that the sample was exposed to the highest force. Samples tested at speed greater than 25 mm/min show a decrease in maximum force.

In samples tested with the hemispherical nose, the maximum force increases with the increase in the number of layers. However, with the increase in speed, the force in the upper surface layer decreases, while the force on the lower surface layer increases.

Displacement damage and damage energy increase as the number of layers increases (Shuaeib & Soden, 1997).

When the graphs in Figure 4.20 are examined, it is seen that they are compared according to the type of impactor. The graphs show that the contact forces of the flat noses are greater than the contact forces of the hemispherical noses.

When the quasi-static loading is applied to the sandwich composite by the hemispherical nose, the shear stress is softer in the first sandwich. The foam is crushing by the contact force after the first sandwich was crushed smoothly. Hemispherical nose has become the maximum shear force and properly punched the material when it passed through the foam and reached the second skin material.

The damage geometry of the perforated sandwich composite by hemispherical nose was obtained more uniformly.

The perforation resistance of the materials varies depending on the nose geometry. The highest puncture resistance is seen at flat noses. Due to the regional perforation resistance in the surface layers of the sandwich structures where quasi-static loading is made with the flat nose, the bending behavior is observed in the upper surface layer (Johnson & Li., 2011).

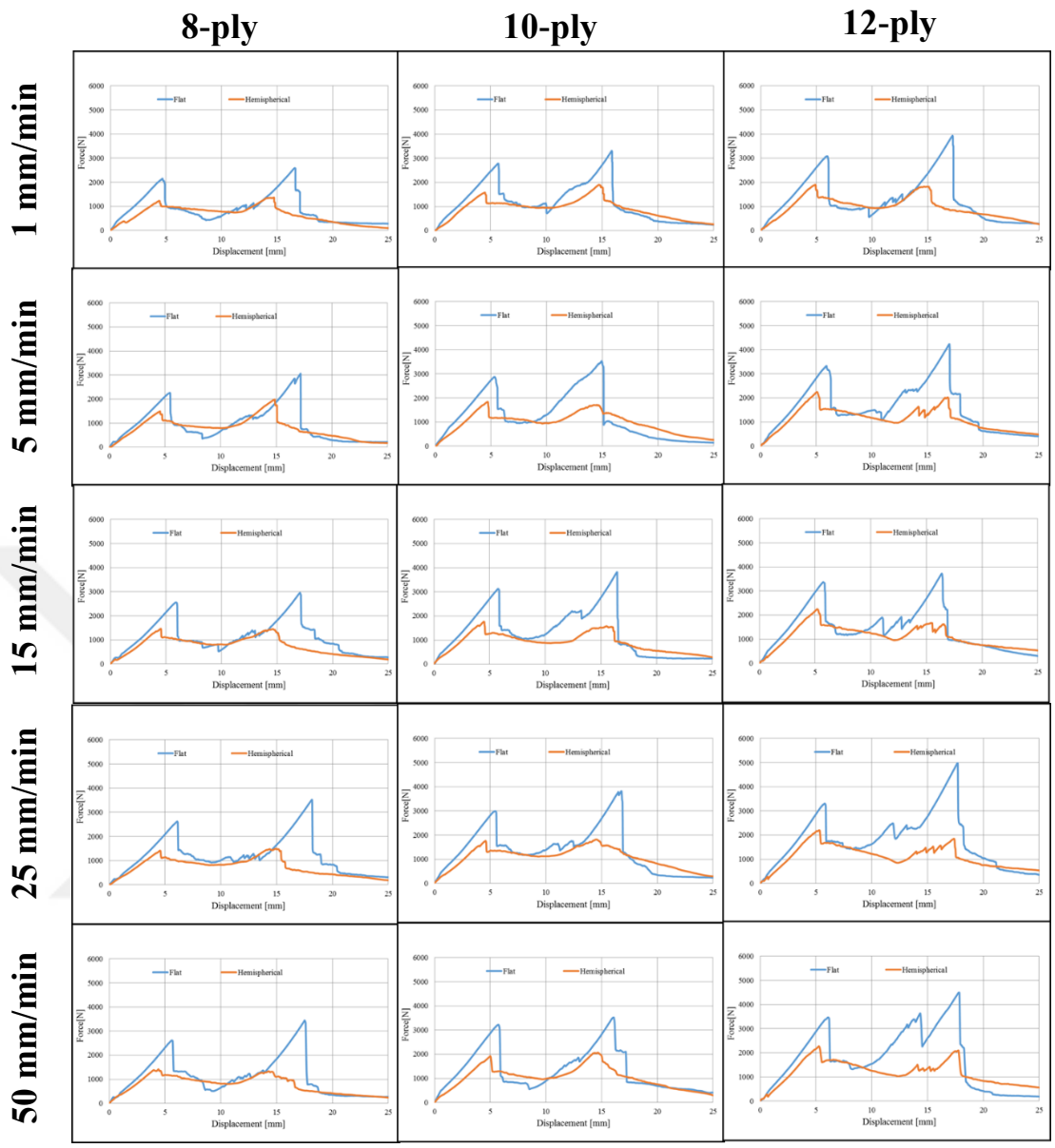


Figure 4.20 Force-displacement graphs according to the noses for different crosshead speeds and ply

It is known that the indentation geometry around the hemispherical noses is an important parameter in reducing fiber damages, matrix damages and delamination (Bulut & Erklig, 2018).

Figure 4.21 shows the force graph according to the crosshead speeds in the quasi-static test.

When the graphs of the 8-layer samples are examined, the maximum force is seen at 25mm/min at the first peak of the graph and in the sample tested with the flat nose. The value of this force was found to be 3514 N. The lowest force of the samples tested with the flat nose was seen at the first peak of the graph at 1 mm/min and its value was found to be 2147 N.

In the samples tested with hemispherical nose, the highest force was seen at the first peak of the graph at 5mm/min speed and its value was found to be 1984 N. It is also seen that the force decreases as the speed increases.

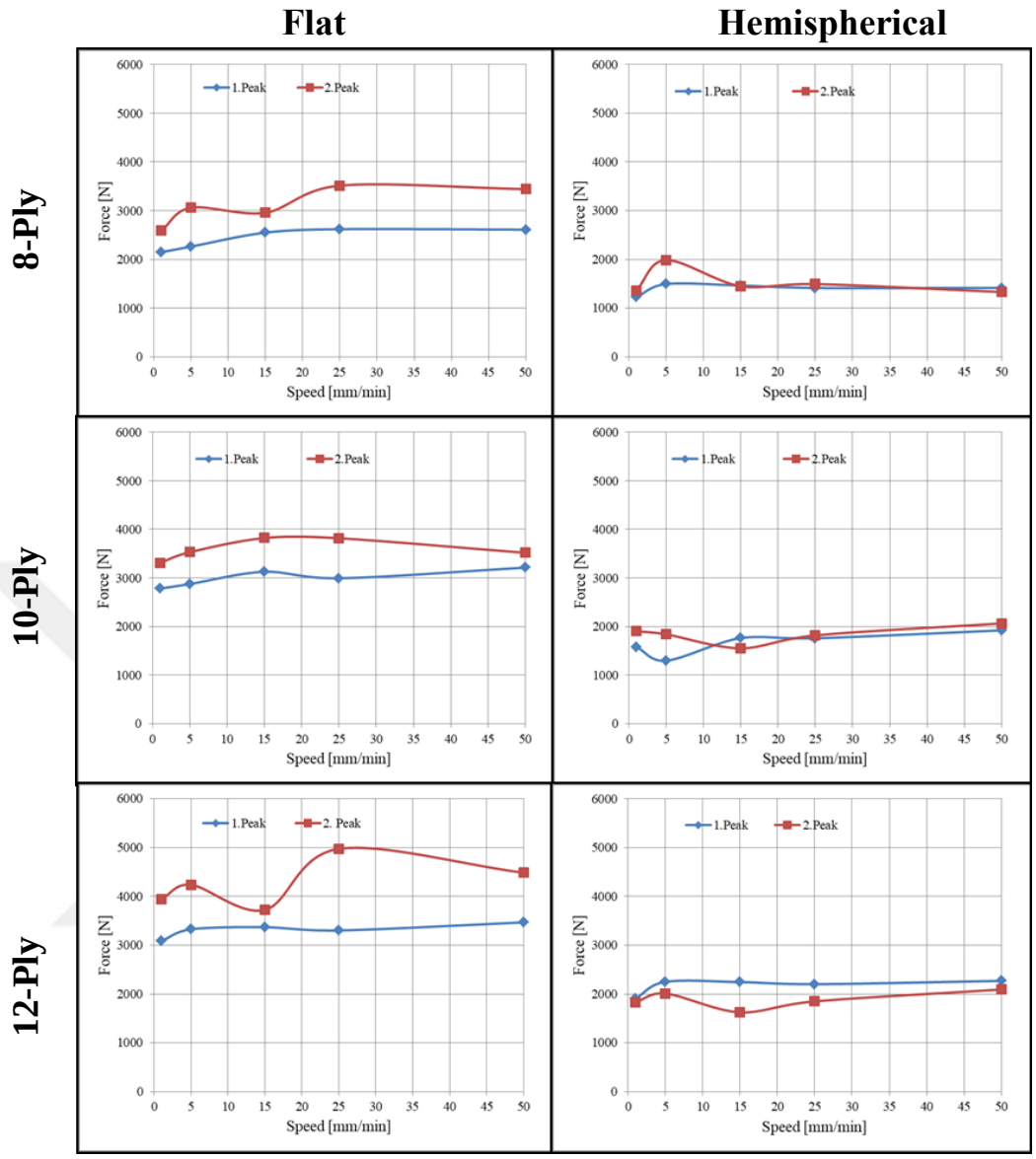


Figure 4.21 Force-speed graphs according to the noses for different ply

The 10-layer sandwich composite specimens tested with the flat nose have the highest strength at the first peak of the graph at 15 mm/min. The value of this force is 3821 N. The force increases as the speed of the flat noses increases up to 50mm/min. The lowest force is seen at the first peak of the graph at 1mm/min speed, and the value of this force is seen as 2780 N.

When the graph of the samples tested with the hemispherical nose is examined, it is seen that the force decreases as the nose velocity increases up to 50 mm/min. The

highest force is 2062 N and it is seen in the first peak of the graph at a speed of 50 mm/min. The lowest force was seen in the first peak of the graph at 5 mm/min and its value was 1295 N.

When the 12-layer sandwich composite graphs are examined, the maximum force for the flat nose is seen at the second peak of the graph at 25 mm/min. The value of the force was found to be 4975 N. The lowest force is seen at the first peak of the graph at 1mm/min and its value is 3084 N.

In the samples tested with a hemispherical nose, the minimum force is seen at the first peak of the graph at a speed of 1mm/min and its value is found as 1829 N. The maximum force was found at the first peak of the graph at 50mm/min, and the value of this force is 2269 N

As the speed increases, it is seen that the forces found in the samples tested with the flat nose and the forces in the samples tested with the hemispherical nose approach each other.

4.2.2 Quasi-Static Damage

Figure 4.22, Figure 4.23 and Figure 4.24 show the damage caused by the quasi-static test with 8, 10 and 12 layer samples at five different speeds and two different nose types, respectively.

In the tests carried out on all three layers, the samples were damaged by fiber and matrix. When the back face of the test specimens made with the flat nose type is examined, tear damage is seen in the surface layers on the back surface. It is seen that the damage on the front surface has sharp corners around the nose.

In specimens exposed with a hemispherical nose, damage to the front surface indicates that the nose circumference is not sharp. Therefore, the hemispherical nose has caused cutting damage on the back face.

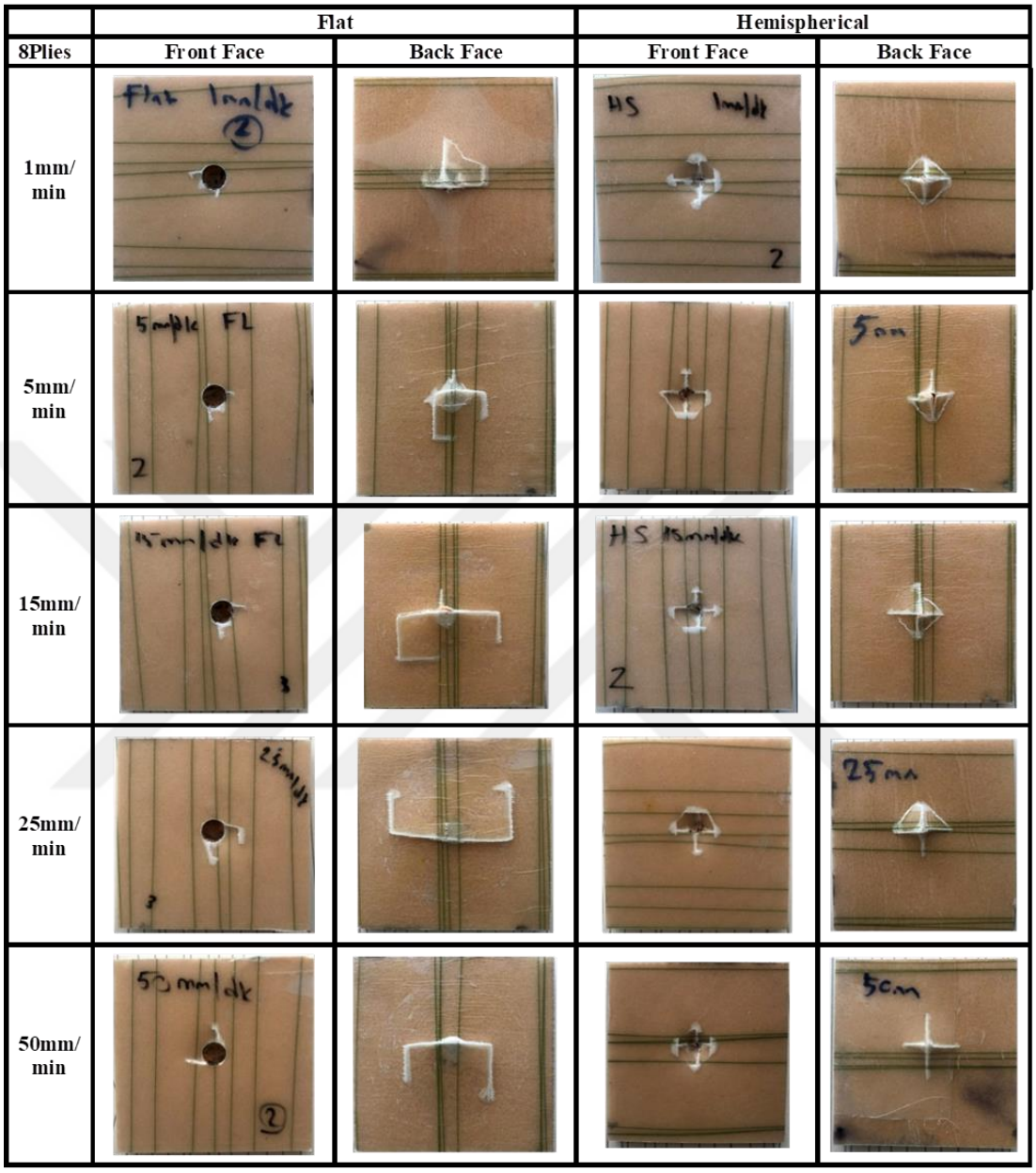


Figure 4.22 Damage after quasi-static test of 8-ply flat, hemispherical noses and sandwich composite samples at different speeds

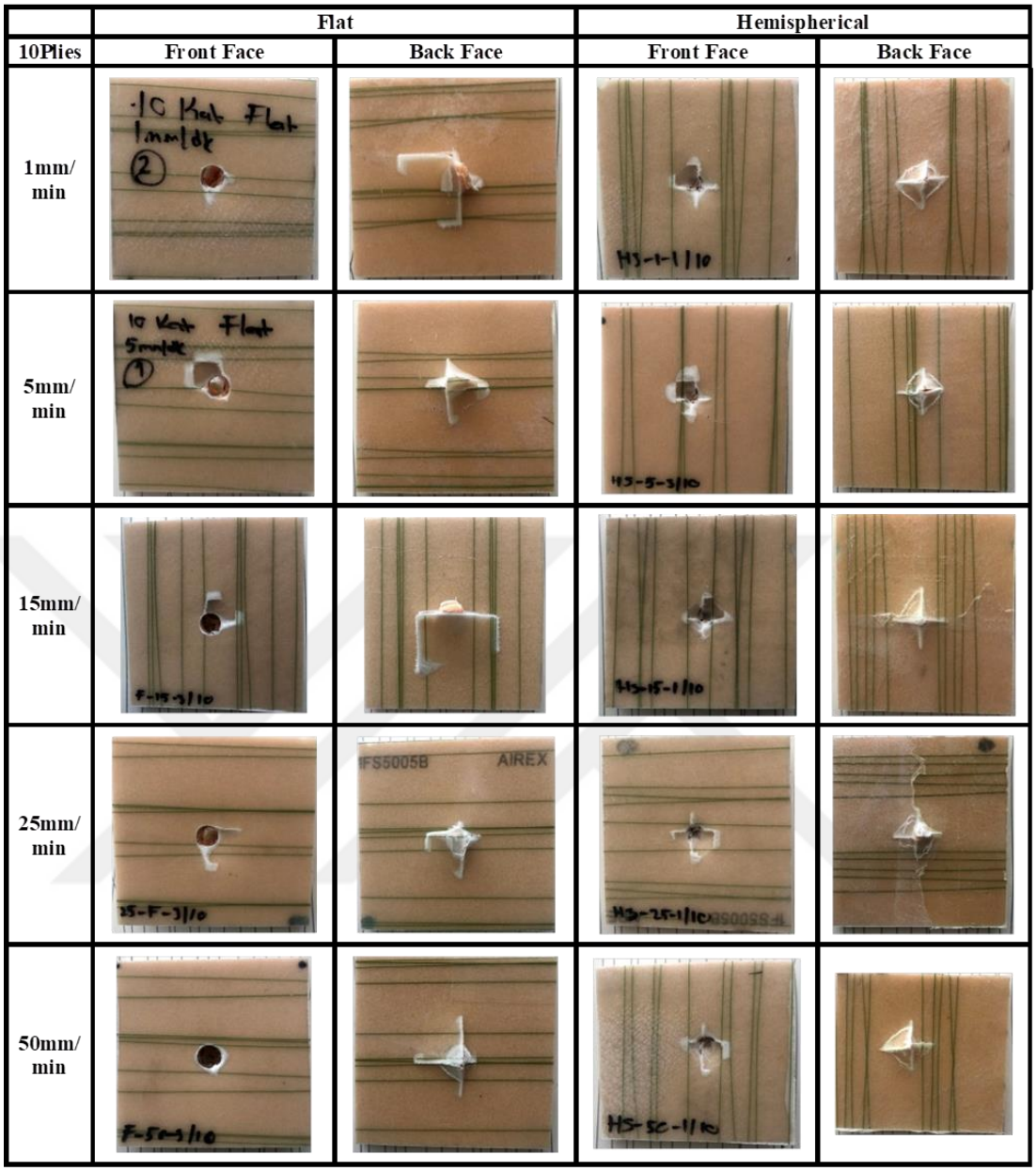


Figure 4.23 Damage after quasi-static test of 10-ply flat, hemispherical noses and sandwich composite samples at different speeds

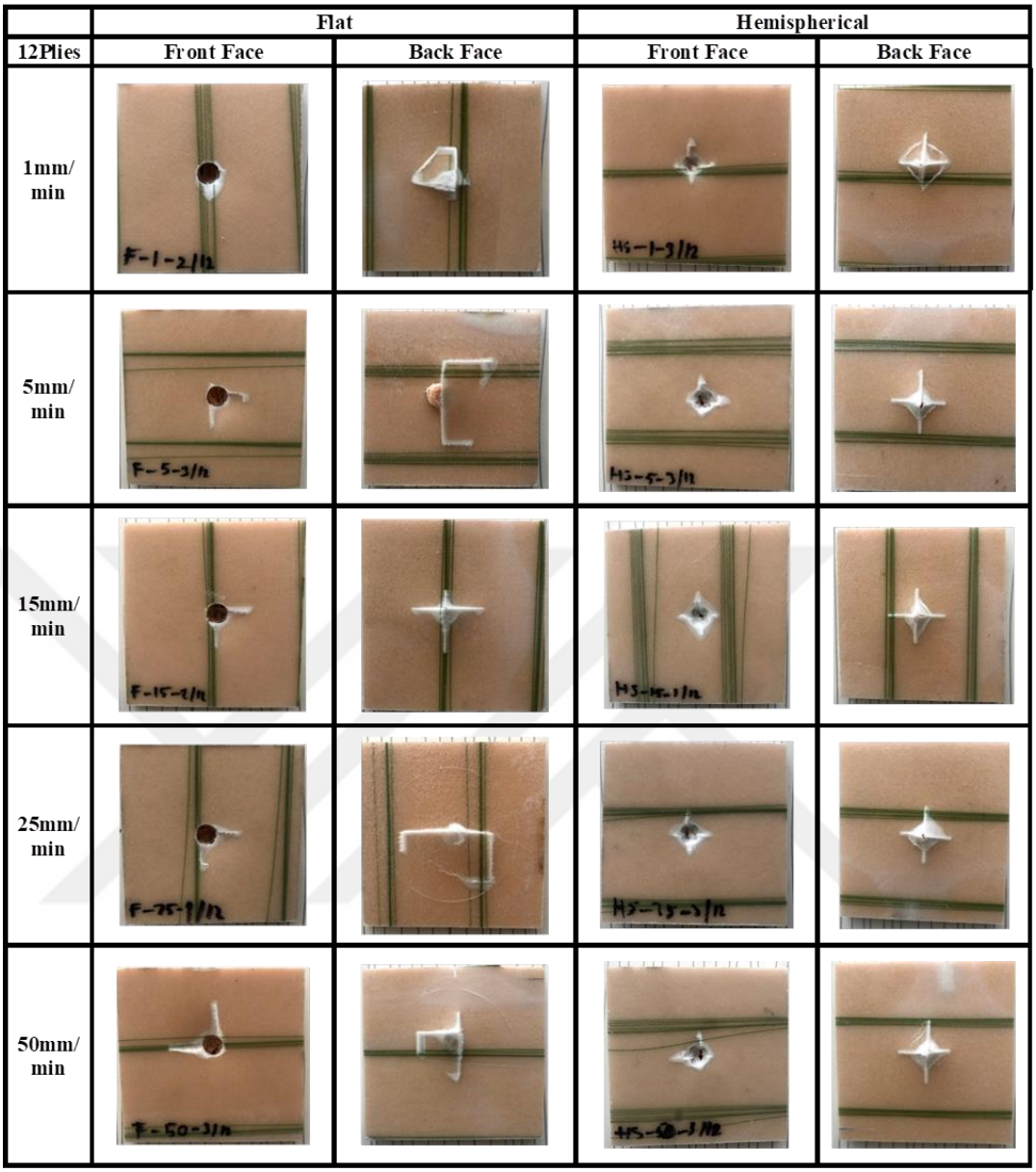


Figure 4.24 Damage after quasi-static test of 12-ply flat, hemispherical noses and sandwich composite samples at different speeds

Delamination and bending damages are seen in the upper surface layer of the samples tested with the flat nose. There is tearing damage on the back surfaces.

Shear damage is observed in the back face-sheet of the samples tested with the hemispherical nose. Delamination and debonding damages are seen on the front surface layer.

CHAPTER FIVE
CONCLUSION

In this thesis, sandwich composites with sheet material as S-glass and core material as PVC foam were produced by VARIM method for three different number of layers as 8, 10 and 12 layers. Low velocity impact tests with flat and hemispherical noses were conducted for impact energies of 80J, 100J and 120J on composite specimens with 100 mm length and 100 mm width. Energy-time and contact force-time graphs were drawn for each experimental group as a result of the tests. Quasi-static punch shear test was also conducted on the same composite samples with five different speeds and two different nose types.

From obtained the results of low velocity impact test, following conclusion can be drawn:

- The maximum contact force increases as the number of layers increases under the same test conditions.
- The maximum contact force of the samples tested with the flat nose was higher than the ones with the hemispherical noses. It can be concluded that the geometry of the specimens tested with the flat nose is sharper than the specimens tested with the hemispherical nose.
- The maximum contact force decreases as the energy level increases in the samples with the same number of layers. As the energy level increases, the material resistance decreases.
- At the energy levels tested, there exist fiber damage in the upper and lower surface layers of the sandwich composites and core damage in the core.
- Damage to the back surface layer of samples tested with the flat nose was seen as tear damage while the back surface layer of samples tested with the hemispherical nose showed shear damage.
- The amount of absorbed energy increases when the number of layers increases.

- The absorbed energy amount of samples with the same number of layers in the flat nose test was more than the amount of energy absorbed in the hemispherical nose test.
- For the same number of layers at different energy levels, it is seen that the amount of absorbed energy for the 100 J impact energy is higher than the other energy levels.
- The increase in the number of layers increases the power applied by the device to the material.
- The amount of force acting on the material with the flat nose is greater than the hemispherical nose.
- Delamination, core fiber debonding and core damage are seen in the tested samples.

The implications of the quasi-static punch test, tested with a 1, 5, 15, 25, 50 mm/min speeds, by flat and hemispherical noses, are as follows:

- The contact force at the hemispherical nose has lower value than the one at the flat nose because of the the difference geometric shapes of noses.
- In tests with the hemispherical nose, the first peak contact forces increases by the increase of nose speed. The second maximum contact force was obtained at 5 mm/min of nose speed. Maximum contact force decreases by the increase of test speed.
- Contact force increases by increase of the number of layer.
- Fiber damage and shear damage occur in the core material.

As a suggestion for further studies, the impact response can be investigated by conical, ogive nose types, differentiation of fabric materials in the layers, and testing at different temperatures. For the quasi-static test, energy absorption capacities can be examined by using different parameters such as conical, ogive nose types and the fibers in the lower surface layer and upper surface layers are composed of different materials. Factors such as the increase in nose diversity, the use of different fiber materials and temperature may be important parameters in these studies.

REFERENCES

Abrate, S. (2011). *Impact engineering of composite structures.* New York: SpringerWien

Akil Hazizan, M. D., & Cantwell, W.J. (2002). The low velocity impact response of foam-based sandwich structures. *Composites Part B, 33,* 193-204.

Al-Shamary, A., Karakuzu, R., & Ozdemir, O. (2016). Low-velocity impact response of sandwich composites with different foam core configurations. *Journal of Sandwich Structures and Materials, 18*(6), 754-768.

Anderson, T., & Madenci, E. (2000). Graphite/epoxy foam sandwich panels under quasi-static indentation. *Engineering Fracture Mechanics, 67*(4), 329-344.

Sandwich Concept. Diab Sandwich Handbook. (2003). Retrieved April 5, 2021, from http://www.diabgroup.com.

Atas, C., & Sevim, C. (2010). On the impact response of sandwich composites with cores of balsa wood and PVC foam. *Composite Structures, 93,* 40-48.

Ayten, A., Ekici, B., & Tasdelen, M. (2019). A numerical and experimental investigation on quasi-static punch-shear test behavior of aramid/epoxy composites. *Polymers and Polymer Composites*, *28*(6) 398-409.

Balaban, A. C., Tee, F. K., & Toygar, E. M. (2019). Low velocity impact behavior of sandwich composite structures with e-glass/epoxy face-sheets and PVC foam. *25th International Conference on Fracture and Structural Integrity, 18,* 577-585.

Balasubramanian, M. (2013). Introduction to composites. *Composite materials and processing* (1-10). London: CRC Press.

Bulut, M., & Erklig, A. (2018). The investigation of quasi-static indentation effect on laminated hybrid composite plates. *Mechanics of Materials, 117,* 225-234.

Campbell, F. C. (2010). *Structural composite materials* (1st Ed.). Ohio: ASM International.

Carlsson, L. A., & Kardomateas, G. A. (2011). *Structural and failure mechanics of sandwich composites*. New York: Springer.

Composite materials handbook vol 6. (2013). Wichita, DC: Society of Automotive Engineers.

Dogan, A., & Arıkan, V. (2017). Low-velocity impact response of E-glass reinforced thermoset and thermoplastic based sandwich composites. *Composites Part B, 17*, 30491-2.

Feng, D., & Aymerich, F., (2020). Effect of core density on the low-velocity impact response of foam-based sandwich composites. *Composite Structures, 239*, 112040.

Flores-Johnson, E. A., & Li, Q. M., (2011). Experimental study of the indentation of sandwich panels with carbon fibre-reinforced polymer face sheets and polymeric foam core. *Composites Part B, 42*, 1212-1219.

Foo, C. C., Chai, G. B., & Seah, L. K. (2006). Quasi-static and low-velocity impact failure of aluminium honeycomb sandwich panels. *Sage Journal, 220*(2), 53-66.

Ghasemnejad, H., Furquan, A. S. M., & Mason, P. J. (2010). Charpy impact damage behaviour of single and multi-delaminated hybrid composite beam structures. *Materials & Design, 31*(8), 3653-3660.

Gomes, F., Agnys, J., Wanderley, F. A. J., Walter, B. F., Isac, P. G., Andrea, L. S., & Wagner, L. P. (2016). Behavior of fiberglass polymer composites under ballistic impact and quasi-static punch shear tests. *Materials Science Forum, 881*, 300-306.

Goren, A., & Atas, C. (2008). Manufacturing of polymer matrix composites using vacuum assisted resin infusion molding. *Archives of Materials Science and Engineering, 34*(2), 117-120.

Gupta, N. (2003). *Characterization of syntactic foams and their sandwich composites: modelling and experimental, approaches*. Phd Thesis, Louisiana State University, United States.

Gustin, J., Joneson, A., Mahifalah, M., & Stone, J. (2005). Low velocity impact of combination Kevlar/carbon fiber sandwich composites. *Composite Structures, 69*, 396-406.

Jordan, B. J., Natio, J. C., & Haque, Z. B. (2013). Quasi-static, low-velocity impact and ballistic impact behavior of plain weave E-glass/phenolic composites. *Journal of Composite Materials, 48*(20), 2505-2516.

Kaw, A. K. (2006). *Mechanics of composite materials* (2nd ed.). Florida: CRC Press.

Lin, C., & Hoo Fatt, M. S. (2006). Perforation of composite plates and sandwich panels under quasi-static and projectile loading. *Journal of Composite Materials, 40*(20), 1801-1840.

Mallick, P. K. (2007). *Fiber-reinforced composites: materials, manufacturing, and design.* London: CRC Press.

Mathivanan, N. R., & Jerald, J. (2010). Experimental investigation of woven e-glass epoxy composite laminates subjected to low-velocity impact at different energy levels. *Journal of Minerals and Materials Characterization and Engineering, 9*(07), 643-652.

Mazumdar, S. (2002). *Composites manufacturing: materials, product, and process engineering.* U.S: CRC Press.

Mohammad, S., & Mohammad, H. P. (2019). Investigation of behaviors of glass/epoxy laminate composites reinforced with carbon nanotubes under quasi-static punch shear loading. *Journal of Sandwich Structures and Materials*, *21*(4), 1535–1556.

Onder, A., & Robinson, M. (2019). Investigating the feasibility of a new testing method for GFRP/polymer foam sandwich composites used in railway passenger vehicles. *Composite Structures*, *233*, 111576

Ozdemir, O., Karakuzu, R., & Al-Shamary, A. (2015). Core-thickness effect on the impact response of sandwich composites with poly (vinyl chloride) and poly (ethylene terephthalate) foam cores. *Journal of Composite Materials*, *49*(11), 1315–1329.

Rana, S., & Fangueiro, R. (2016). *Advanced composite materials for aerospace engineering processing, properties and applications* (1 Edition). London: Elsevier.

Rajak, D. P., Pagar, P. P., Menezes, P. L., & Linul, E. (2019). Fiber-reinforced polymer composites: Manufacturing, properties, and applications. *Polymers*, *11*(10), 1667.

Reddy, T. Y., Wen, H. M., Reid, S. R., & Soden, P. D. (1998). Penetration and perforation of composite sandwich panels by hemispherical and conical projectiles. *Journal of Pressure Vessel Technology*, *120*(2), 186-194.

Safri, S. N. A., Sultan, M. T. H., Yidris, N., & Mustapha, F. (2014). Low velocity and high velocity impact test on composite materials. *The International Journal of Engineering and Science*, *3*(9), 50-60.

Sakly, A., Laksimi, A., Kebir, H., & Benmedakhen, S. (2016). Experimental and modelling study of low velocity impacts on composite sandwich structures for railway applications. *Engineering Failure Analysis*, *68*, 22-31.

Salami, S. J. (2013). Experimental study on quasi-static response of multi-layer sandwich composite structures. *World Academy of Science, Engineering and Technology International Journal of Mechanical and Mechatronics Engineering, 7*(5).

Sarioglu, R., Karakuzu, R., & Kandas H. (2020) Effects of crosshead speed and penetrator shape on the punch shear behaviors of sandwich composites. *4th International Students Science Congress*, 369-374.

Schubel, P. M., Luo, J. J., & Daniel, I. M. (2005). Low velocity impact behavior of composite sandwich panels. *Composites Part A, 36,* 1389-1396

Shuaeib, F. M., & Soden, I. D. (1997). Indentation failure of composite sandwich beams. *Composites Science and Technology, 57*(9-10), 1249-1259

Staab, G. H. (2015). *Laminar composites* (2. Edition). London: Elsevier.

Ude, A. U., Ariffin, A. K., & Azhari, C. H. (2013). An experimental investigation on the response of woven natural silk fiber/epoxy sandwich composite panels under low velocity impact. *Fibers and Polymers*, *14*(1), 127-132

Xiao, J. R., Gama, B. A., & Gillespie Jr, J. W. (2007). Progressive damage and delamination in plain weave S-2 glass/SC-15 composites under quasi-static punch-shear loading. *Composite Structures*, *53*, 182-196.

Yahaya, R. S. M., Sapuan, S. M., Jawaid, M., Leman, Z., & Zainudin, E. S. (2014). Quasi-static penetration and ballistic properties of kenaf–aramid hybrid composites. *Materials and Design*, *63*, 775-782.

Yuan, L., Hai, W., Costas, S., Tristan, L., & Robert, C. (2015). Progressive damage in satin weave carbon/epoxy composites under quasi-static punch-shear loading. *Polymer Testing*, *41*, 82-91.

Zhou, J., Hassan, M. Z., Guan, Z., & Cantwell, J. (2012). The low velocity impact response of foam-based sandwich panels. *Composites Science and Technology, 78*, 1781-1790.